Sinking fate and carbon export of zooplankton fecal pellets: insights from time-series sediment trap observations in the northern South China Sea

Hanxiao Wang[1], Zhifei Liu[1], Jiaying Li[1], Baozhi Lin[1], Yulong Zhao[1], Xiaodong Zhang[1], Junyuan Cao[1], Jingwen Zhang[1], Hongzhe Song[1], and Wenzhuo Wang[1]

[1]State Key Laboratory of Marine Geology, Tongji University, Shanghai, 200092, China

Correspondence to: Z. Liu (lzhifei@tongji.edu.cn)

Abstract. The sinking of zooplankton fecal pellets is a key process in the marine biological carbon pump, facilitating the export of particulate organic carbon (POC). Here, we analysed~~analyzed~~ zooplankton fecal pellets collected by two time-series sediment traps deployed on mooring TJ-A1B in the northern South China Sea (SCS) from May 2021 to May 2022. The results show a seasonal variability in both fecal pellet numerical (FPN) flux and fecal pellet carbon (FPC) flux, with peaks in November to April and June to August. It implies that the fecal pellet flux is largely regulated by the East Asian monsoon system. Vertical analysis further shows that FPN and FPC fluxes are higher at 1970 m than at 500 m water depth, with larger pellets occurring in the deeper water, indicating a significant influence of mesopelagic/bathypelagic zooplankton community and lateral transport on deep-sea ~~fecal pellet carbon~~ FPC export. However, the biovolume of amorphous pellets decreases significantly from 500 m to 1970 m water depth, implying that these fecal pellets are broken and fragmented during the sinking process, possibly due to zooplankton grazing and disturbance by deep-sea currents. The contribution of fecal pellets to total POC export in the northern SCS is in average 3.4% and 1.9% at 500 m and 1970 m water depths, respectively. This study highlights that the sinking fate of fecal pellets is regulated by marine primary productivity~~marine surface productivity~~, deep-sea dwelling zooplankton community, and deep-sea currents in the tropical marginal sea, thus providing a new perspective for exploring the carbon cycle in the world ocean.

1 Introduction

The marine biological carbon pump (BCP) is a collection of processes whereby marine organisms mediate the transfer of carbon from the atmosphere to the deep ocean. Marine organisms inhabiting the upper water column can fix atmospheric CO_2 through photosynthesis, producing particulate organic carbon (POC) in the epipelagic~~euphotic~~ zone. Subsequently, a series of processes transport the POC, including phytoplankton cells, zooplankton fecal pellets, moults~~molts~~, carcasses, and aggregates, from surface to deeper layers of the ocean, representing a significant component of the global carbon cycle (Fowler and Knauer, 1986; Steinberg and Landry, 2017). As a key process of~~in~~ the BCP, zooplankton feed on phytoplankton and other materials and pack them into fecal pellets, thereby reducing ~~fecal pellets can reduce~~ the dissolution and degradation of organic matter

during the sinking process and subsequently increase the particle sinking flux in the mesopelagic and bathypelagic zones (Wilson et al., 2008; Turner, 2015). During the sinking process, most zooplankton fecal pellets are susceptible to being ingested by other zooplankton or degraded by bacteria. Several studies have revealed that the concentration of fecal pellets in the deep sea is significantly lower compared to the production rate of fecal pellets in the surface waters, and the presence of amorphous fecal pellets (mostly fragmented pellets) has been observed, indicating significant consumption during the sinking process (Juul-Pedersen et al., 2006; Wilson et al., 2008; Goldthwait and Steinberg, 2008; Kobari et al., 2010, 2016; Stukel et al., 2013; Miquel et al., 2015). Copepods are the primary consumers of fecal pellets, with retention rates ranging from 30% to 98% (Svensen et al., 2012; Turner, 2015). Noji et al. (1991) categorized copepod behaviourbehavior in fecal pellet consumption into three different types: coprorhexy (fragmentation of fecal pellets), coprophagy (ingestion of fecal pellets), and coprochaly (loosening of fecal pellets). These processes are thought to reduce the carbon export of fecal pellets in the deep sea (Noji et al., 1991). However, the repackaging of larger zooplankton inhabiting the mesopelagic zones, accompanied by their in -situ production of large fecal pellets, may contribute to an increasing flux of deep-sea fecal pellets (Urrère and Knauer, 1981; Shatova et al., 2012; Manno et al., 2015; Belcher et al., 2017). In addition, diurnal vertical migration results in active subsurface transport, and thus, zooplankton mediated injection pump is considered an important mechanism for BCP to increase deep-sea carbon export flux (Boyd et al., 2019). The efficiency of the BCP depends on the carbon export flux and the retention of remineralized carbon in the deep ocean. As a key component of the carbon cycle, fragmentation, decomposition, and repackaging of fecal pellets may affect the POC export and regulate the efficiency of the BCP.

Numerous studies have been conducted in the global ocean to explore the biogeochemical mechanisms of zooplankton fecal pellets during production, sinking, degradation, and recycling processes of zooplankton fecal pellets (González et al., 2000; Gleiber et al., 2012; Belcher et al., 2017; Le Moigne, 2019). Changes in the characteristics and fluxes of fecal pellets at varying depths can be utilized as an indicator of zooplankton behaviour (Wilson et al., 2008). Previous studies have observed obvious clear differences in fecal pellet flux with increasing water depth, mostly showing a decreasing trend (Viitasalo et al., 1999; Wexels Riser et al., 2007). However, in certain regions, such as the Northeast Pacific, Mediterranean Sea, Sargasso Sea, and Southern Ocean, fecal pellet fluxes tend to increase in the deep layer (Urrère and Knauer, 1981; Fowler et al., 1991; Wassmann et al., 2000; Shatova et al., 2012; Manno et al., 2015; Belcher et al., 2017). This variation in the trend of fecal pellet flux with water depth is influenced by the composition of local zooplankton community and efficiency of the BCP. Different shapes and sizes of fecal pellets have different sinking rates, which contribute differently to the POC export (Wilson et al., 2008; Manno et al., 2015; Turner, 2015; Steinberg and Landry, 2017; Qiu et al., 2018). In the high-latitude eutrophic seas, fecal pellets tend to exhibit a high contribution to the total POC flux (Juul-Pedersen et al., 2006; Wilson et al., 2008; Manno et al., 2015). However, the contribution in the subpolar mesotrophic seas and low-latitude oligotrophic seas is significantly lower. Pilskaln and Honjo (1987) reported that fecal pellets account for less than 5–10% of sinking flux in tropical and subtropical regions. Taylor (1989) also reported that fecal pellets contribute a minimal fraction (6%) of the POC flux in the central North Pacific. Roman and Gauzens (1997) suggested that the contribution of fecal pellets to the total carbon flux was quite small in the tropical Pacific, and that most fecal pellets produced in the surface waters were ingested during sinking.

The South China Sea (SCS) is considered as an oligotrophic tropical sea and a source of CO_2 (Su, 2004; Cao et al., 2020).

65 Owing to its unique geographical and physicochemical characteristics, the organic carbon flux and its regulatory processes in the SCS are subject to significant spatiotemporal variability. Previous studies have investigated the composition and flux of sinking POC in the northern and central SCS, which vary with the East Asian monsoon system. Notably, the peak occurrence of sinking POC has been observed during the northeast monsoon period (Chen et al., 1998; Liu et al., 2007; Li, H. et al., 2017; Zhang et al., 2019, 2022; Blattmann et al., 2018, 2019). Based on the C/N ratio and stable/radiocarbon isotope analyses, the

70 vertical vector of modern POC turns out to be 87% ± 4% of the sinking POC in the northern SCS, with the lateral vector accounting for the remaining 13% (Zhang et al., 2022). The contribution of laterally supplied POC becomes more significant with increasing depth, which is largely derived from lithogenic organic carbon transported by the deep-sea currents and resuspension of slope sediments (Blattmann et al., 2018; Zhang et al., 2022). In the southern SCS, Li et al. (2022) conducted the first study of zooplankton fecal pellet characteristics, numerical fluxes, and carbon fluxes in the tropical marginal sea,

75 showing that fecal pellets contribute 0.4–30.0% to the total POC flux. Despite the dominance of marine-origin organic carbon in sinking POC in the northern SCS, detailed studies of the rapidly sinking particles are sparse, and the contribution of fecal pellets to the total carbon flux remains uncertain. To better understand the efficiency and biogeochemical cycling of the BCP in the northern SCS, we collected sinking zooplankton fecal pellets from mesopelagic and bathypelagic waters using two time-series sediment traps to quantify the role of fecal pellets in POC export. By analysing analyzing the shape, quantity, internal

80 composition, and carbon content of zooplankton fecal pellets, we gained more specific insights into the sinking fate of these pellets in tropical marginal seas and highlighted the importance of fragmentation during the sinking process in determining the carbon flux transferred to the deep sea.

2 Study area

The SCS is a large marginal sea with an area of about $3.5×10^6$ km^2 and an average depth of about 1350 m (Wang and Li, 2009).

85 The study area is located in the northern SCS, where a warm and humid southwest monsoon prevails in summer (June to August), while a dry and cold northeast monsoon prevails in winter (November to April) (Chu and Wang, 2003) (Fig. 1). The hHydrological system of the northern SCS is complex due to the seasonal shift of the East Asian monsoon winds and the interplay of waters from the Kuroshio Current (Su, 2004; Caruso et al., 2006). Surface circulation of the northern SCS also shows a seasonal shift from a large cyclonic gyre in winter to a weak cyclonic gyre in summer (Su, 2004). Contour currents

90 have been found to dominate sediment transport processes on the deep-sea slope at 1600–2400 m water depth, transporting Taiwan-sourced sediments westward (Zhao et al., 2015; Liu et al., 2010, 2016). A cCombination of strong winter winds, water mixing, and surface cooling in the northern SCS drives winter convective overturning, leading to higher primary productivity during the winter monsoon than during other periods (Liu et al., 2002; Chen, 2005; Tseng et al., 2005). Rainfall in the northern SCS is seasonally variable, with increased rainfall during the summer (Zhang et al., 2019). Typhoons, mesoscale eddies, and

95 other dynamical processes are also well developed in the northern SCS (Su, 2004; Wang and Li, 2009).
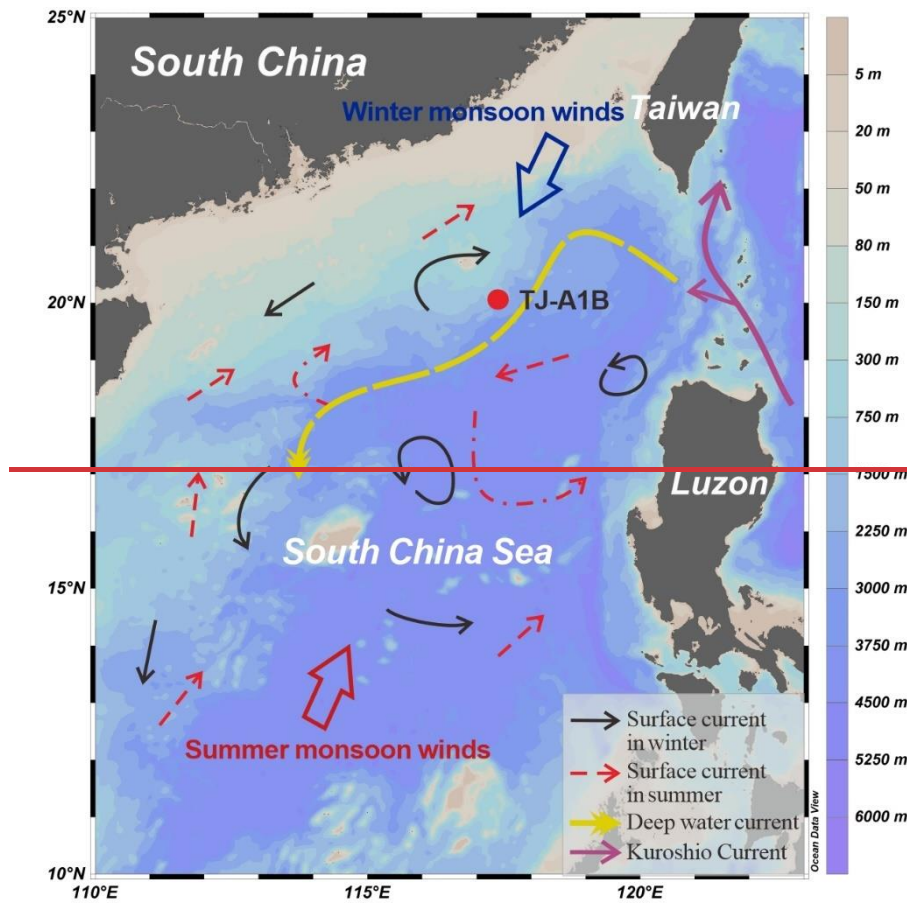
Figure 1. Monsoon and current systems in the South China Sea (SCS) (after Liu et al., 2016). Location of the sediment trap mooring TJ-A1B is indicated. Ocean Data View software was used to generate the map (Schlitzer, 2023).

100 Zooplankton species in the northern SCS mainly include Hydromedusae, Siphonophorae, Pteropoda, Ostracoda, Copepoda, Amphipoda, Euphausiacea, Chaetognatha, Appendiculariae, Thaliacea, and larvae (Fig. 2a; Li et al., 2021; Gong et al., 2017). Among these, copepods have the largest number of species, contributing 30% of the total identified species (Ren et al., 2021; Ge et al., 2021). Copepods are also the most abundant group, contributing about 80% of the total abundance, followed by ostracods and chaetognaths (Fig. 2a). Zooplankton abundance is the highest between 0–100 m water depth and consistently

105 decreases with increasing depth (Fig. 2b; Gong et al., 2017; Li et al., 2021). The average zooplankton biomass is 35 mg m^{-3}, with a slight increase at 350–600 m water depth (Gong et al., 2017). Below 300 m, there is a noticeable increase in the proportion of copepods to the total abundance, with some copepod species (including *Calanoides carinatus*, *Bradyiditus armatus*, *Chiridius gracilis*, and *Euchirella curticauda*) only found at 450–1000 m water depth (Du et al., 2014; Li et al., 2021).

23 Material and Methods

2.1 Study area

The SCS is a large marginal sea with an area of about 3.5×10^6 km^2 and an average depth of about 1350 m (Wang and Li, 2009). The study area is located in the northern SCS, where a warm and humid southwest monsoon prevails in summer (June to August), while a dry and cold northeast monsoon prevails in winter (November to April) (Chu and Wang, 2003) (Fig. 1). The hydrological system of the northern SCS is complex due to the seasonal shift of the East Asian monsoon winds and the interplay of waters from the Kuroshio Current (Su, 2004; Caruso et al., 2006). Surface circulation of the northern SCS also shows a seasonal shift from a large cyclonic gyre in winter to a weak cyclonic gyre in summer (Su, 2004). Contour currents have been found to dominate sediment transport processes on the deep-sea slope at 1600–2400 m water depth, transporting Taiwan-sourced sediments westward (Zhao et al., 2015; Liu et al., 2010, 2016). A combination of strong winter winds, water mixing, and surface cooling in the northern SCS drives winter convective overturning, leading to higher primary productivity during the winter monsoon than during other periods (Liu et al., 2002; Chen, 2005; Tseng et al., 2005). Rainfall in the northern SCS is seasonally variable, with increased rainfall during the summer (Zhang et al., 2019). Typhoons, mesoscale eddies, and other dynamical processes are also well developed in the northern SCS (Su, 2004; Wang and Li, 2009).
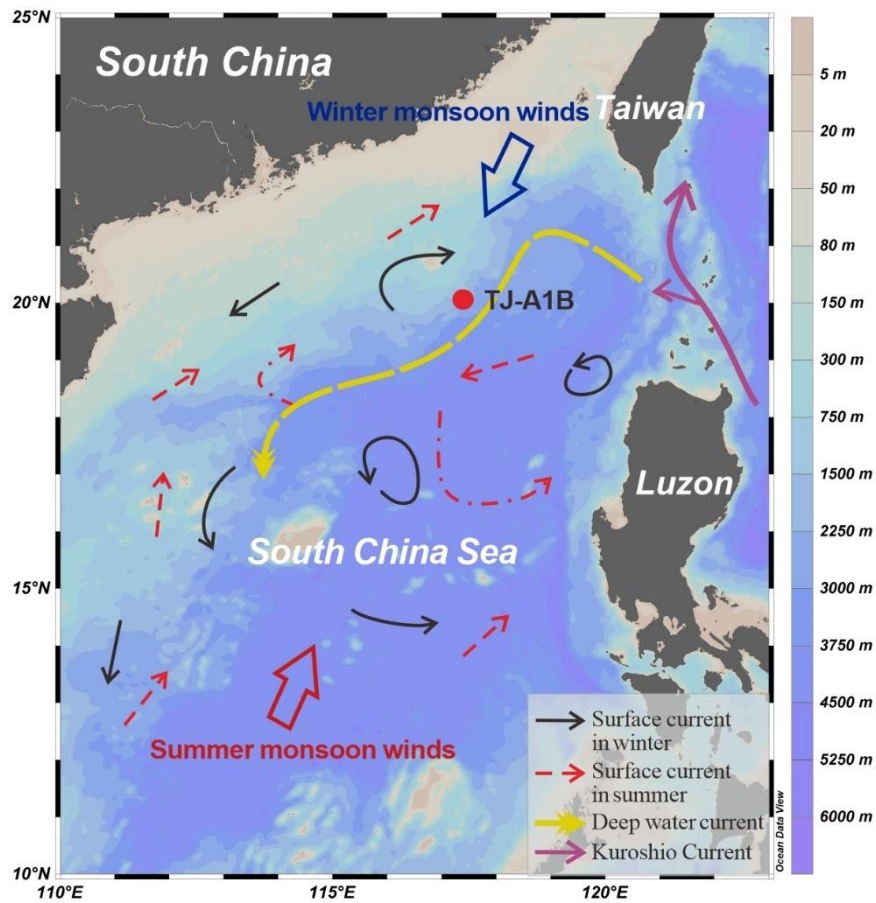
Figure 1. Monsoon and current systems in the South China Sea (SCS) (after Liu et al., 2016). Location of the time-series sediment trap mooring TJ-A1B is indicated. Ocean Data View software was used to generate the map (Schlitzer, 2023).

Zooplankton species in the northern SCS mainly include Hydromedusae, Siphonophorae, Pteropoda, Ostracoda, Copepoda, Amphipoda, Euphausiacea, Chaetognatha, Appendiculariae, Thaliacea, and larvae (Fig. 2a; Li et al., 2021; Gong et al., 2017). Among these, copepods have the largest number of species, contributing 30% of the total identified species (Li, K. et al., 2017; Ren et al., 2021; Ge et al., 2021). Copepods are also the most abundant group, contributing about 80% of the total abundance, followed by ostracods and chaetognaths (Fig. 2a). Zooplankton abundance is the highest between 0–100 m water depth and consistently decreases with increasing depth (Fig. 2b; Gong et al., 2017; Li et al., 2021). The average zooplankton biomass is 35 mg m^{-3}, with a slight increase at 350–600 m water depth (Gong et al., 2017). Below 300 m, there is a noticeable increase in the proportion of copepods to the total abundance, with some copepod species (including *Calanoides carinatus*, *Bradyiditus armatus*, *Chiridius gracilis*, and *Euchirella curticauda*) only found at 450–1000 m water depth (Du et al., 2014; Li et al., 2021).

Furthermore, on a seasonal scale, zooplankton abundance in the northern SCS increases significantly during the winter monsoon period, while it declines during the inter-monsoon period (Li et al., 2004; Li et al., 2021).
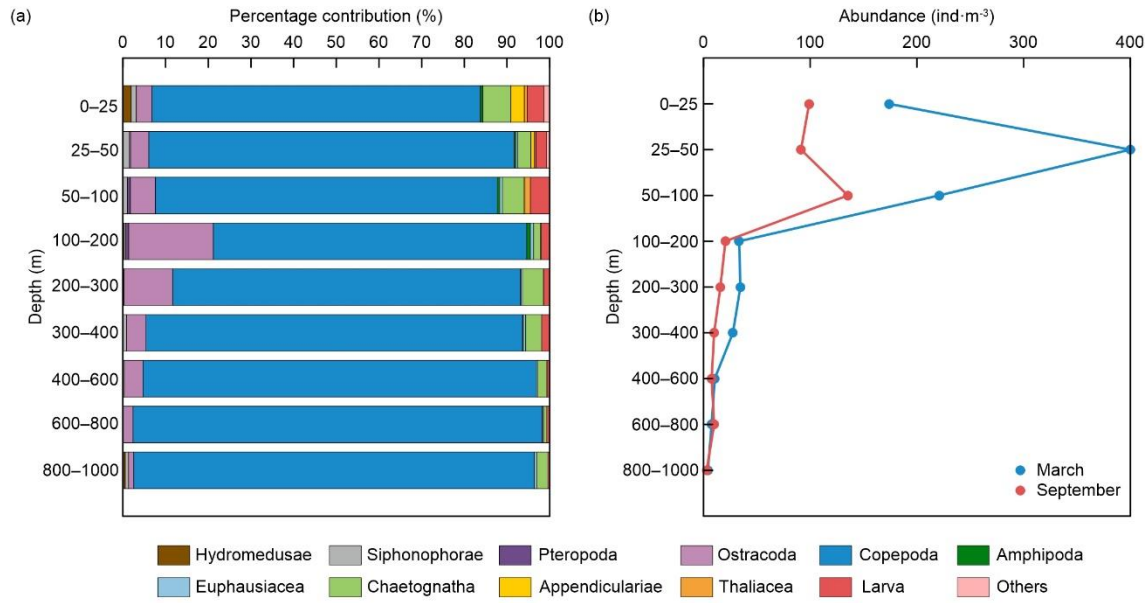
Figure 2. Vertical distribution of (a) species richness percentage and (b) total abundance of zooplankton from 0 to 1000 m
145 depths in the northern SCS. Data from Li et al. (2021).

23.21 Sediment trap deployment

Samples were collected by time-series sediment traps (McLane Parflux Mark78H-21 sediment trap) deployed on mooring TJ-A1B (20.06°N, 117.39°E, 2000 m water depth) in the northern SCS (Fig. 1). Two traps (UP and DW) were deployed at 500 m
150 and 1970 m water depths, respectively, each with a sampling area of 0.5 m². Samples were collected at 18-day intervals from May 2021 to May 2022 (except for the first sample, which covered only three days), resulting in a total of 42 samples (21 samples for each trap). Prior to deployment of the traps, each sample bottle was pre-filled with 0.6 g (for the trap at 500 m) or 0.3 g (for the trap at 1970 m) $HgCl_2$, along with 33.3 g NaCl per 1000 ml of deionized water to prevent microbial activity and ensure the reliability of organic geochemical analysis.

155 ## 23.32 Sample analysis

The samples were wet sievedseived using a 1 mm mesh to remove swimmers. The small fractions (<1 mm) were then equally aliquoted using a splitter, and one wet portion was used for the analysis of zooplankton fecal pellets. POC content and flux were determined using the methods outlined in detail by Li et al. (2022). The wet samples were filtered through a 20 μm Nitex © mesh, followed by rinsing on a gridded petri dish. These samples were examined under a Zeiss Stemi 508 stereomicroscope

160 coupled to a Zeiss Axiocam 305 digital camera. Fecal pellets were photographed and counted by shape to obtain the fecal pellet numerical (FPN) flux (Li et al., 2022). Pellets were classified into four shapes: ellipsoidal, cylindrical, spherical, and amorphous. Biovolumes of the first three fecal pellet shapes were calculated from the formulas for an ellipsoid, cylinder, and sphere (Sun and Liu, 2003), while the biovolume of amorphous fecal pellets was estimated through best-fit ellipsoid calculations (Kumar et al., 2010). The fecal pellet biovolume was then converted to carbon content to determine the fecal pellet

165 carbon (FPC) flux and its contribution to the POC flux, by using the conversion factor of 0.036 mg C mm^{-3} measured in the southern SCS (Li et al., 2022), which is similar to the conversion factor commonly used in tropical and subtropical marginal seas (Urban-Rich et al., 1998; Kobari et al., 2010).

Fecal pellets selected from eight samples at two different depths were prepared for scanning electron microscopy (SEM) and energy-dispersive spectrometry (EDS) to identify their internal structure and to determine elemental composition. 6–7 fecal

170 pellets of different shapes (ellipsoidal, cylindrical, spherical, and amorphous) and aggregates were randomly selected from each sample.

2~~3~~.4~~3~~ Hydrological parameters

To investigate the environmental factors regulating the sinking and export of fecal pellets, we analysed ~~analyzed~~ several relevant physical and biogeochemical parameters. For daily wind speed (10 m zonal and meridional components of surface

175 wind), data were derived from the Atmospheric Composition Reanalysis 4 product (https://ads.atmosphere.copernicus.eu/cdsapp#!/dataset/cams-global-reanalysis-eac4), with a spatial resolution of 0.25°×0.25°. Daily sea surface temperature (SST) data were retrieved from the Copernicus Climate Change Service (https://cds.climate.copernicus.eu/cdsapp#!/dataset/satellite-sea-surface-temperature), which provides SST data with a horizontal resolution of 0.05°×0.05°. For daily ocean mixed layer depth (MLD) defined by potential density anomaly and

180 surface water velocity, data were retrieved from the Operational Mercator global ocean analysis and forecast system (https://data.marine.copernicus.eu/product/GLOBAL_ANALYSISFORECAST_PHY_001_024/description), with spatial resolutions of 0.25°×0.25° and 0.083°×0.083°, respectively. Daily net primary production (PP) data of biomass expressed as carbon per unit volume in sea water with a spatial resolution of 0.25°×0.25° were obtained from the Operational Mercator Ocean biogeochemical global ocean analysis and forecast system

185 (https://data.marine.copernicus.eu/product/GLOBAL_ANALYSIS_FORECAST_BIO_001_028). Daily precipitation data with a horizontal resolution of 1.0°×1.0° were provided by the Global Precipitation Climatology Project (https://cds.climate.copernicus.eu/cdsapp#!/dataset/satellite-precipitation).

34 Results

34.1 Fecal pellet characteristics

190 Microscopic analysis of the time-series sediment trap samples revealed fecal pellets of various shapes (ellipsoidal, cylindrical, spherical, and amorphous). All shapes were found both at 500 m (Fig. 3a) and 1970 m (Fig. 3b). Among them, ellipsoidal, cylindrical, and spherical pellets were intact with smooth edges, while amorphous pellets were degraded with broken edges. Notably, their peritrophic membranes were partially absent. Fecal pellets were often brown in appearance~~., which were~~ ~~significantly different between the two depths.~~ Ellipsoidal, cylindrical, and spherical pellets sizes were larger at 1970 m,

195 whereas amorphous fecal pellets sizes were larger at 500 m (Fig. 3, detailed photographs can be found in Supplementary Figs. S1–S21). In addition to zooplankton fecal pellets, a number of transparent and flocculent aggregates were also present in the samples, which were more common in the winter samples (Fig. 3, Figs. S1–S21).

Figure 3. Light microscopy photographs of four morphological types of zooplankton fecal pellets and aggregates collected

200 from (a) 500 m and (b) 1970 m water depths of time-series sediment trap mooring TJ-A1B in the northern SCS.

The internal components of the fecal pellets were mainly composed of diatoms, e.g., *Coscinodiscus* (Fig. 4a, ~~and 4~~e), *Thalassionema* (Fig. 4h), *Hemiaulus* (Fig. 4g), and *Nitzschia* (Fig. 4g), as well as coccoliths (Fig. 4d) and lithogenic particles (Figs. 4h, ~~and~~ 5b). In contrast, the aggregates had a looser structure, and consisted mainly of radiolarians, diatoms, sponge

205 spicules, and foraminifers (Fig. 4i). The major elements composing ~~of~~ the fecal pellets were O, Si, C, and Ca, with minor proportions of Al and K, indicating that terrigenous minerals such as quartz and clay minerals may also be important components of fecal pellets (Figs. 4h, ~~and~~ 5b).
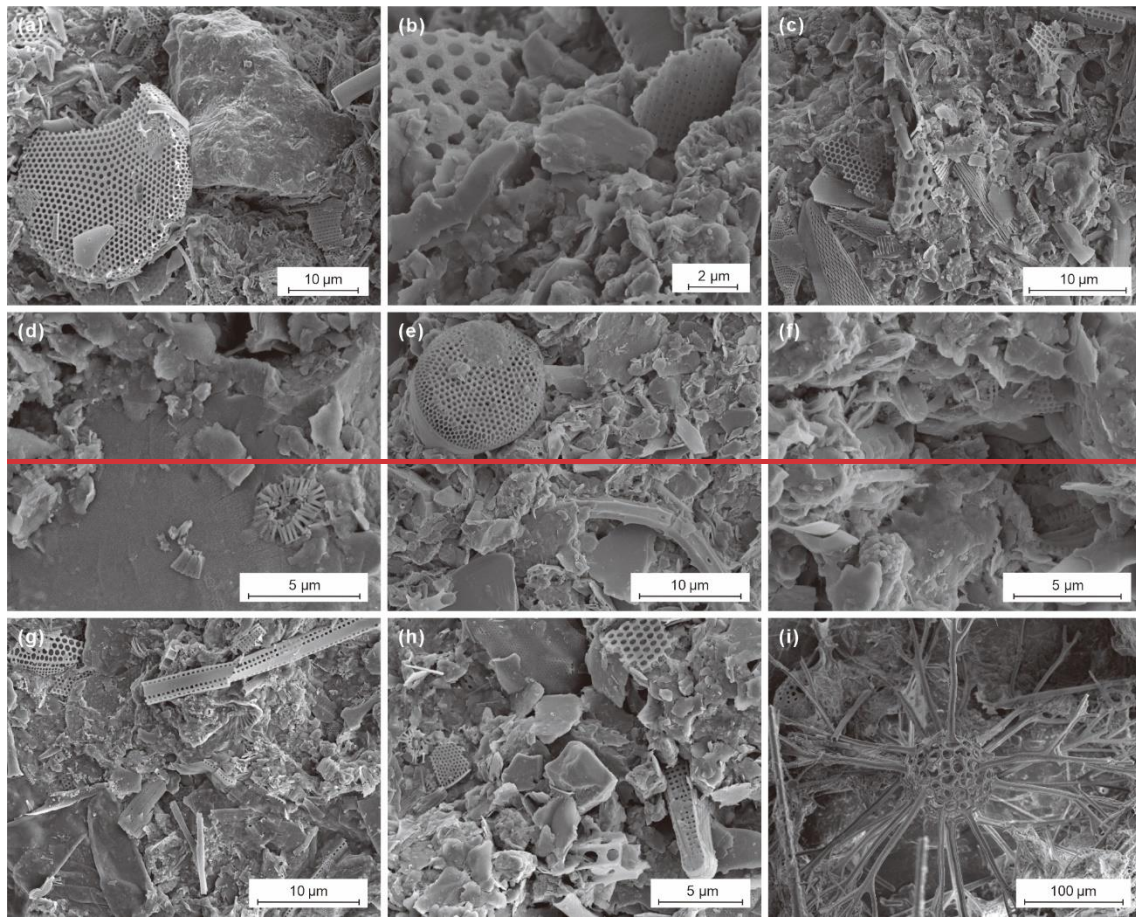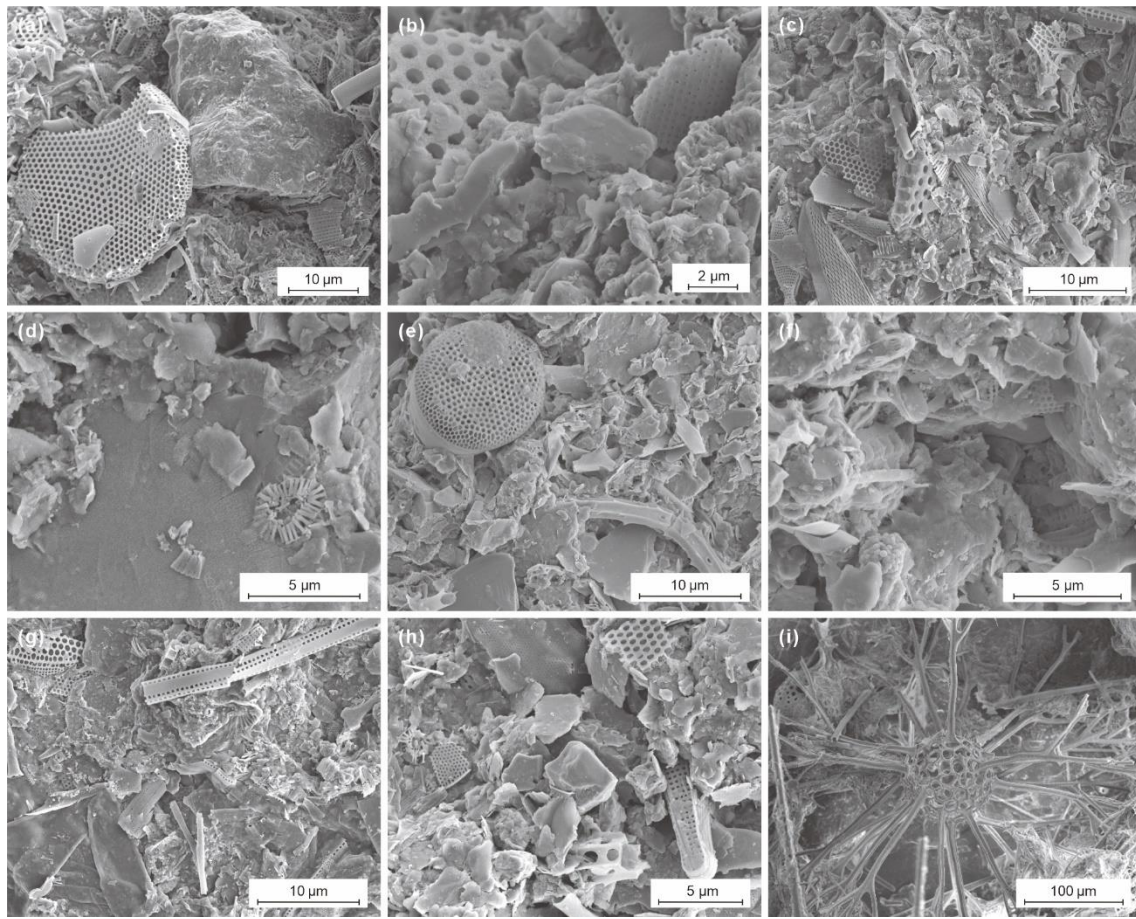
210 **Figure 4.** Scanning electron microscopy (SEM) observations of internal components of zooplankton fecal pellets and aggregates collected from the time-series sediment trap mooring TJ-A1B in the northern SCS: (a, b) ellipsoidal pellet, (c, d) cylindrical pellet, (e, f) spherical pellet, (g, h) amorphous pellet, and (i) aggregates.
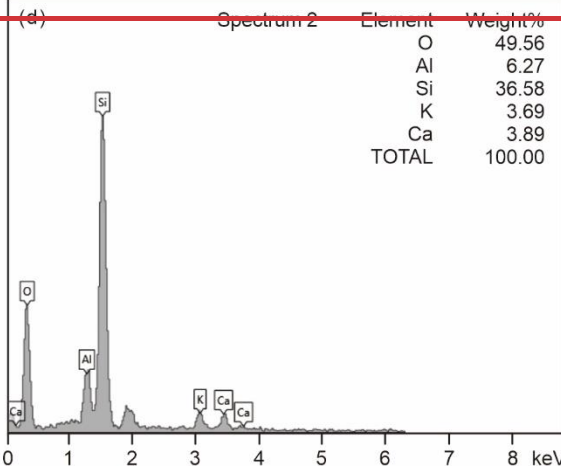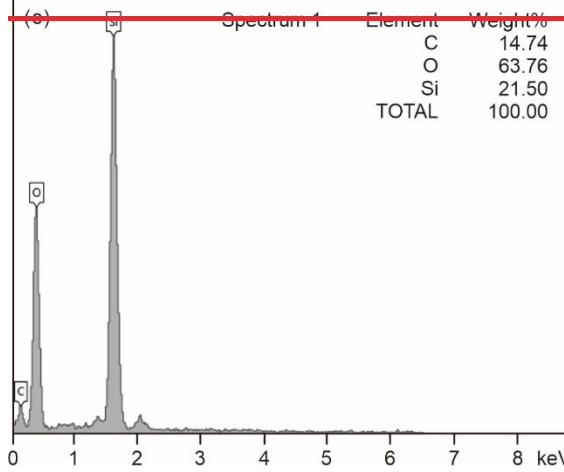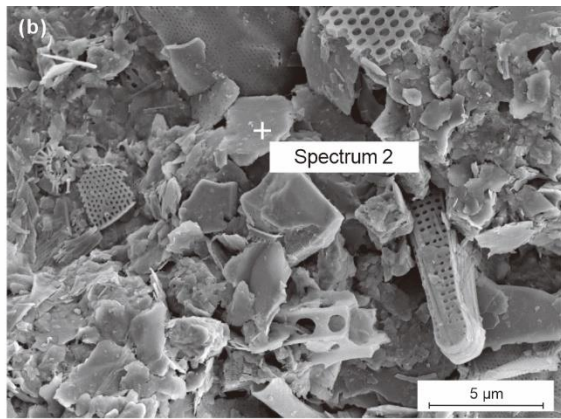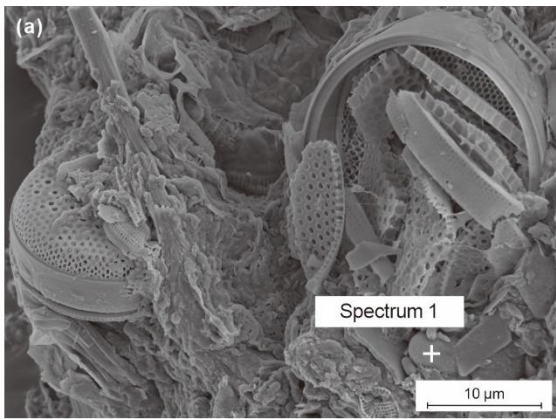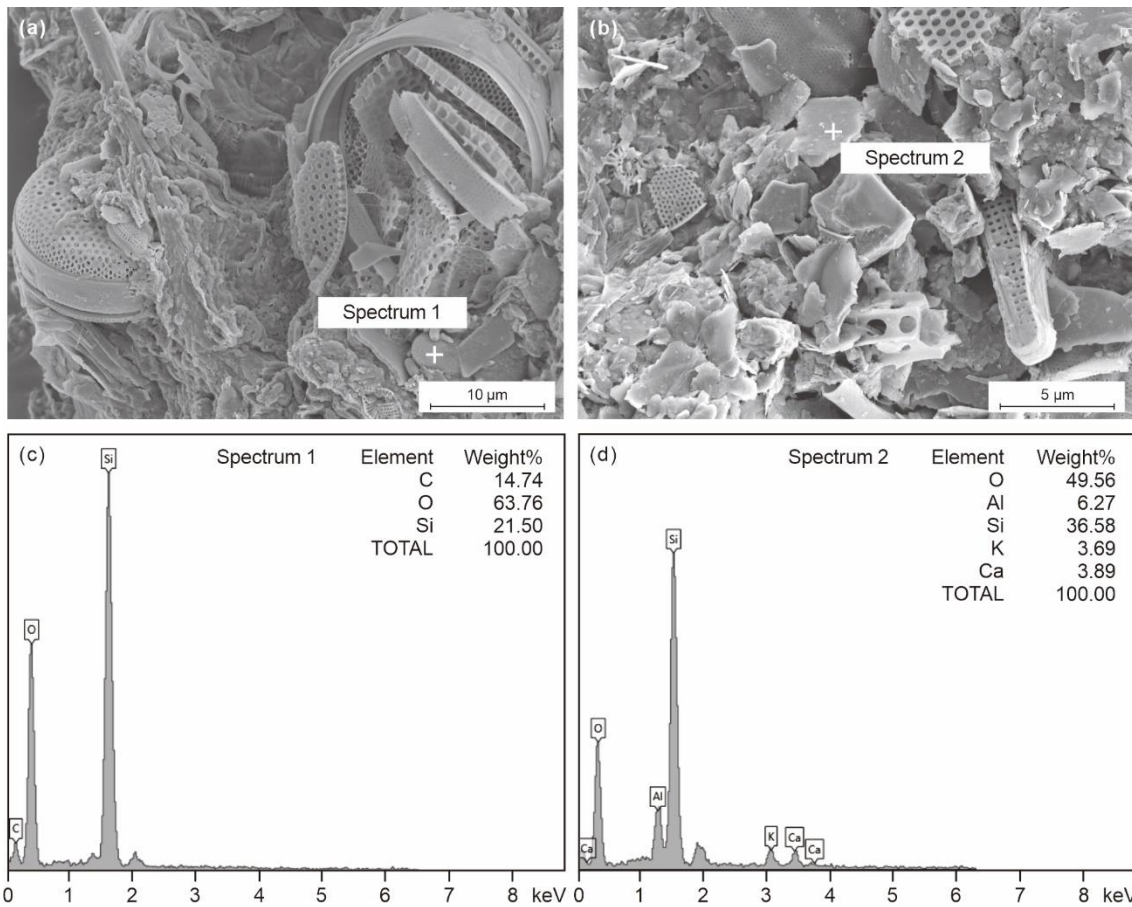
Figure 5. SEM coupled EDS analysis for internal structure and elemental composition of zooplankton fecal pellets in the time-series sediment trap mooring TJ-A1B in the northern SCS. Panels (a) and (c) for one fecal pellet, and panels (b) and (d) for another fecal pellet.

Fecal pellets varied considerably in biovolume among the four types (Table 1). Ellipsoidal pellets had average biovolumes of 1.96 and 3.02×10^6 μm^3 at 500 and 1970 m depth, respectively. The average biovolumes of cylindrical pellets were 13.31×10^6 μm^3 at 500 m and 13.55×10^6 μm^3 at 1970 m, which were 10 times larger than other pellet types. Spherical pellets were the smallest, with a mean biovolume of only 0.90×10^6 μm^3. The biovolume of amorphous pellets ranged from 0.04 to 35.89×10^6 μm^3 and the average value was two times larger at 500 m (2.23×10^6 μm^3) than at 1970 m (0.92×10^6 μm^3). Two patterns of biovolume change from 500 m to 1970 m were observed for different fecal pellet types. Specifically, the average biovolume of ellipsoidal, cylindrical, and spherical pellets increased from 500 m to 1970 m, where the average biovolume of amorphous pellets decreased at 1970 m to only half of that at 500 m. At 500 m, the average biovolume of ellipsoidal, cylindrical, and spherical pellets was higher during June to August and December to February. The average biovolume of amorphous pellets

was elevated from December to April at 500 m. Whereas, at 1970 m, the seasonal variation in biovolume for all shape was not significant.

230

Table 1. Biovolume, numerical flux, numerical percentage, carbon flux, and carbon percentage of four types of zooplankton fecal pellets in the time-series sediment trap mooring TJ-A1B in the northern SCS.

Depth (m)	Fecal pellet type	Number measured	Biovolume ($\times 10^6\,\mu m^3$)	Numerical flux ($\times 10^3\,m^{-2}\,d^{-1}$)	Numerical percentage (%)	Carbon flux (mg C $m^{-2}\,d^{-1}$)	Carbon percentage (%)
500	Ellipsoidal	1278	0.03–49.56	0.05–1.42	20–58	0.0004–0.0184	3–47
			1.96 ± 4.53	**0.38 ± 0.36**	**37 ± 11**	**0.0053 ± 0.0046**	**26 ± 11**
	Cylindrical	501	0.09–118.39	0–0.21	0–19	0–0.1028	0–90
			13.31 ± 19.28	**0.07 ± 0.06**	**8 ± 5**	**0.0103 ± 0.0217**	**29 ± 19**
	Spherical	540	0.01–4.81	0–0.52	0–21	0–0.0032	0–9
			0.90 ± 1.02	**0.11 ± 0.11**	**11 ± 5**	**0.0009 ± 0.0008**	**4 ± 2**
	Amorphous	1331	0.04–35.89	0.15–0.74	15–75	0.0017–0.0138	7–82
			2.23 ± 4.27	**0.34 ± 0.14**	**45 ± 16**	**0.0063 ± 0.0028**	**40 ± 18**
	Total	3650	0.03–118.39	0.22–2.52	100	0.0021–0.1148	100
			3.46 ± 8.98	**0.91 ± 0.59**		**0.0228 ± 0.0238**	
1970	Ellipsoidal	1981	0.05–96.19	0.28–2.51	36–62	0.0048–0.0802	35–82
			3.02 ± 8.01	**1.15 ± 0.66**	**50 ± 6**	**0.0256 ± 0.0199**	**51 ± 11**
	Cylindrical	628	0.07–294.90	0.04–0.45	3–12	0.0033–0.0681	14–53
			13.55 ± 25.97	**0.19 ± 0.13**	**8 ± 2**	**0.0156 ± 0.0158**	**29 ± 12**
	Spherical	897	0.04–10.92	0.08–0.91	7–21	0.0009–0.0075	1–15
			0.90 ± 1.47	**0.34 ± 0.24**	**14 ± 4**	**0.0031 ± 0.0020**	**7 ± 3**
	Amorphous	1481	0.04–12.68	0.20–1.19	14–43	0.0015–0.0191	2–26
			0.92 ± 1.84	**0.60 ± 0.31**	**28 ± 8**	**0.0054 ± 0.0038**	**13 ± 6**
	Total	4987	0.04–294.90	0.60–4.57	100	0.0108–0.1697	100
			3.34 ± 11.30	**2.28 ± 1.24**		**0.0497 ± 0.0360**	

Bold values are the average and standard deviation of each above ranges.

235 **3****.2 Fecal pellet flux**

Fecal pellet numerical (FPN) flux and fecal pellet carbon (FPC) flux at different depths were summarized in Table 1 and Fig. 6. FPN flux varied considerably throughout the year, from a minimum of 216 pellets $m^{-2}\,d^{-1}$ in May to a maximum of 2518

pellets m^{-2} d^{-1} in December at 500 m, while at 1970 m, this value spanned a range of 597–4573 pellets m^{-2} d^{-1}, with the minimum value occurring in October and the maximum in May. FPC flux varied between 0.0021 and 0.1148 mg C m^{-2} d^{-1} at 500 m

240 (Table 1; Fig. 6b). At 1970 m, the range was 0.0108 to 0.1697 mg C m^{-2} d^{-1} (Table 1; Fig. 6d). The most apparent temporal trend in the FPN and the FPC fluxes was a distinct seasonal variation (Fig. 6). There was a double seasonal peak, with a primary (higher) peak ~~in~~ from November to ~~-~~April and a secondary peak from~~in~~ June to ~~-~~August (Fig. 6). In particular, the FPC flux increased slightly in June 2021 before declining sharply over the next 3 months (Fig. 6), and then increasing again with a primary peak from November to April. An anomalously high value of FPC flux was detected at 500 m ~~in~~ during April

245 to ~~-~~May 2022, caused by a large increase in cylindrical pellets (Fig. 6b). Moreover, both FPN and FPC fluxes increased from 500 m to 1970 m, with values at 1970 m twice as high as those measured at 500 m (Table 1).
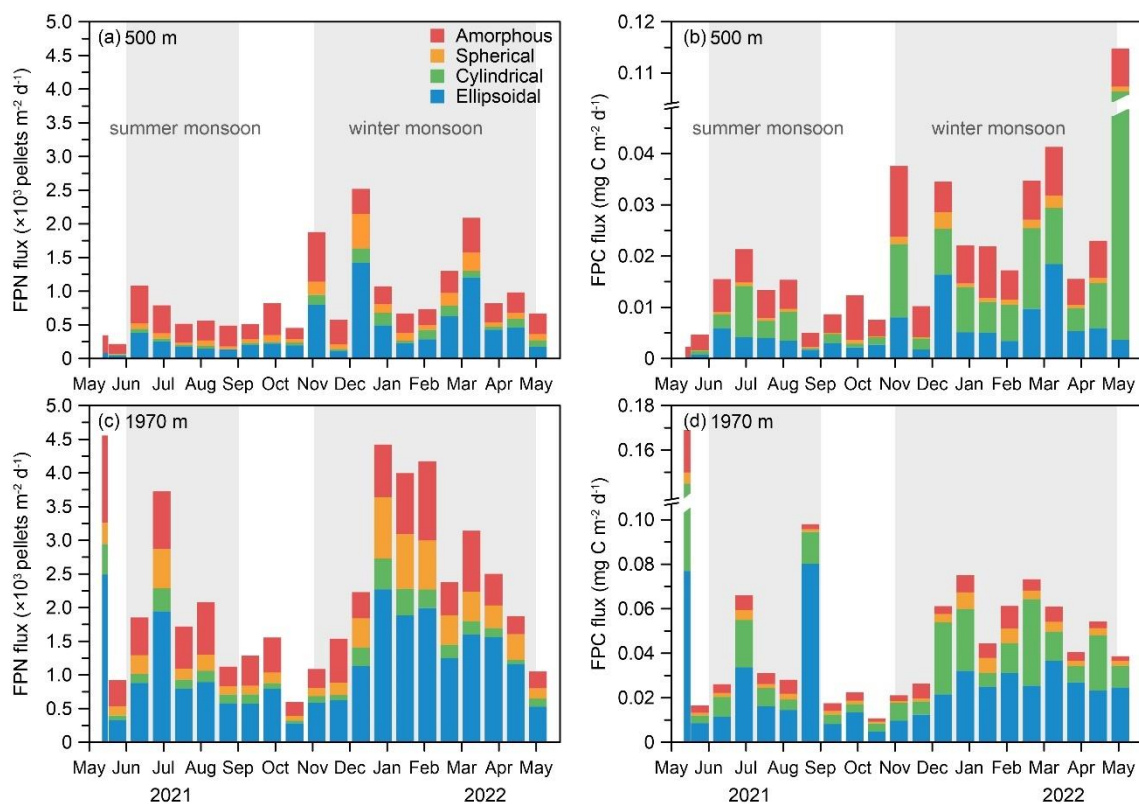
Figure 6. Temporal variations of FPN and FPC fluxes of fecal pellets at the time-series sediment trap mooring TJ-A1B in the northern SCS. (a) FPN flux at 500 m; (b) FPC flux at 500 m; (c) FPN flux at 1970 m; (d) FPC flux at 1970 m.

250

The total fecal pellet flux consisted of four morphological pellet types, with each type making a distinct contribution to the total FPN and FPC fluxes (Table 1; Fig. 6). Typically, ellipsoidal and amorphous pellets dominated the numerical flux, accounting for 80% of the total FPN flux. Cylindrical and spherical pellets were minor contributors to the FPN flux. In terms

of the dominance of different types of fecal pellets, there were notable differences between the two depths (Table 1; Fig. 6).

255 Amorphous pellets accounted for around 45% of the FPN flux at 500 m, while ellipsoidal pellets became most prominent at 1970 m. Cylindrical and spherical pellets had a relatively constant but low numerical percentage. Regarding FPC flux, amorphous pellets contributed on average 40% of the total FPC flux at 500 m, followed by cylindrical pellets (on average 29%) with larger size compared to the other types, despite their relatively low numerical flux. Ellipsoidal pellets contributed on average 26%, while spherical pellets contributed only 4%. At 1970 m, ellipsoidal and cylindrical pellets dominated the FPC

260 flux throughout the time series. Carbon percentage of amorphous pellets declined to 2–26%, while spherical pellets still remained the lowest (1–15%) (Fig. 6b, and 6d). Notably, ellipsoidal, cylindrical, and spherical pellets exhibited higher FPN and FPC fluxes at 1970 m than at 500 m. However, amorphous pellets had lower carbon fluxes and carbon percentages at 1970 m due to their significantly lower biovolumes.

34.3 Contribution of fecal pellets to total POC flux

265 The POC flux in the northern SCS ranged from 0.11 to 5.31 mg C m^{-2} d^{-1} at 500 m, while it varied between 1.08 and 8.19 mg C m^{-2} d^{-1} at 1970 m (Fig. 7). A high seasonal variability of the POC flux was observed, with maxima in the winter monsoon period and minima in the inter-monsoon period at two depths (Fig. 7). This seasonal variation of the POC flux matched that of the FPC flux, with a higher peak from November to April, a lower peak from June to August, and a minimum value from September to October (Fig. 7). In addition to the temporal variation, the POC flux also varied significantly at different depths.

270 On average, the POC flux at 500 m was only ~50% of that measured at 1970 m, and the minimum POC flux at 1970 m was one order of magnitude higher than that observed at 500 m.

The contribution of fecal pellets to the POC flux (FPC/POC ratio) ranged from 0.3% to 15.7% at 500 m, with the highest contribution occurring in during April to -May (Fig. 7). The FPC/POC ratio was generally low from May to July (<4%) and fluctuated between 1%–8% from August to December. During the winter monsoon period, this ratio remained fairly constant

275 (~2%), and then it increased sharply in from April to -May. At 1970 m, the FPC/POC ratio varied from 0.5% to 5.7%, with a smaller range compared to that of 500 m. It was generally low except for May and August 2021(5.7% and 4.8%, respectively), and the minimum occurred in January 2022. In general, the FPC/POC ratio is relatively higher at 500 m and lower at 1970 m, with average percentages of 3.4% and 1.9%, respectively (Fig. 7).
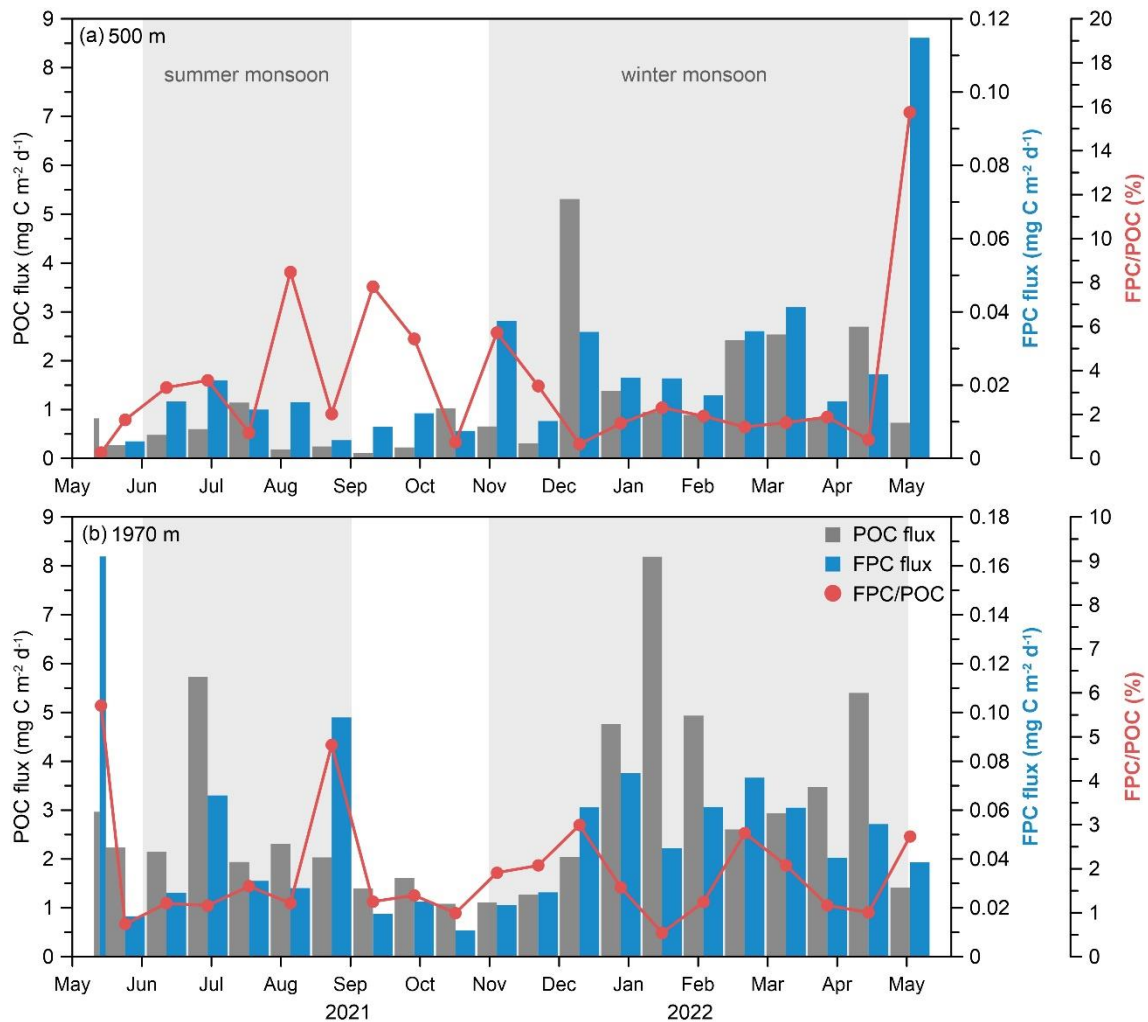
280 **Figure 7.** POC flux, FPC flux and FPC/POC ratio at water depths of (a) 500 m and (b)1970 m at the time-series sediment trap mooring TJ-A1B in the northern SCS.

Positive linear correlations were observed between the POC flux and the FPC flux (Fig. 8a). Sample TJ-A1B21-UP21, which contained a substantial quantity of cylindrical fecal pellets measuring up to 1.5 mm in size but low POC flux, was removed
285 from the fitted relationship. Meanwhile, there were negative linear relationships between the POC flux and the FPC/POC ratio (%) (Fig. 8b). HoweverBesides, the negative linear relationship was weaker at 1970 m compared to 500 m.
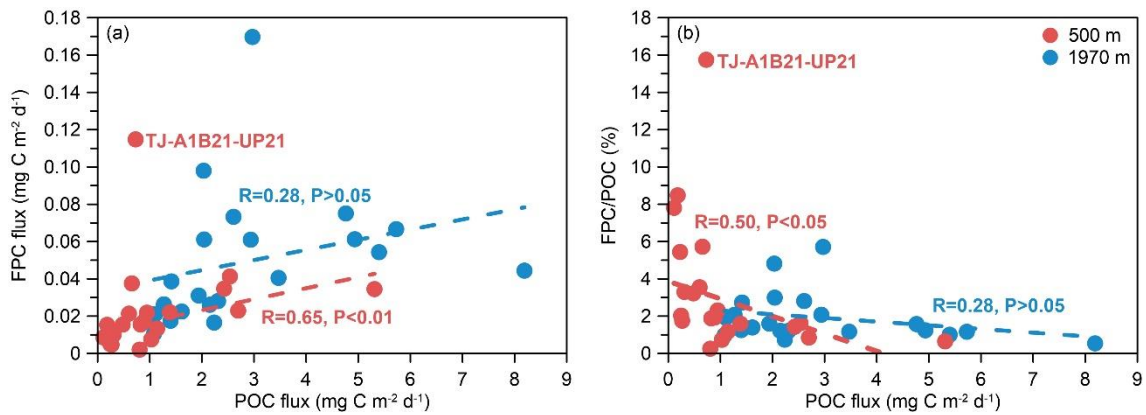
Figure 8. Correlation plots of (a) POC flux versus FPC flux (b) POC flux versus FPC/POC ratio of the time-series sediment trap mooring TJ-A1B in the northern SCS.

290

3.4 Hydrological conditions

Southwest winds prevailed in the study area from June to September and northeast winds from late October to May (Fig. 9a). During the observation period, wind speed ranged from 0.2 to 19.8 m s^{-1}. Wind speed was low during the inter-monsoon period (6.4 ± 3.2 m s^{-1}) and increased in late October, reaching up to 8–10 m s^{-1} in winter (Fig. 9a). Sea surface temperature (SST)
295 varied between 24 to 31°C, with an average of 27 ± 2°C, and showed distinct seasonal variation (Fig. 9b). SST was generally high during summer and autumn (>28°C), declined continuously after November, reaching a minimum (24°C) in January and March. Mixed layer depth (MLD) ranged from 11 to 95 m, with an average value of 35 ± 22 m (Fig. 9c). MLD was typically shallow (<40 m) during spring and summer, increased in autumn and reached its maximum (95 m) in late December (Fig. 9c). Primary productivity (PP) varied between 4 to 34 mg m^{-3} d^{-1} with an average value of 12 ± 6 mg m^{-3} d^{-1} (Fig. 9d). PP showed
300 a weak peak in December (25 mg m^{-3} d^{-1}) and a strong peak in February. Precipitation ranged from 0 to 32 mm d^{-1} with an average value of 3 mm d^{-1} (Fig. 9e). Precipitation throughout the year was concentrated during June to October (7 ± 8 mm d^{-1}), with a maximum value occurred in August and low precipitation during winter (1 ± 2 mm d^{-1}). Sea water velocity fluctuated throughout the year (0.01–0.38 m s^{-1}), averaging 0.17 ± 0.07 m s^{-1} (Fig. 9f). The maximum value occurred during the winter monsoon period.
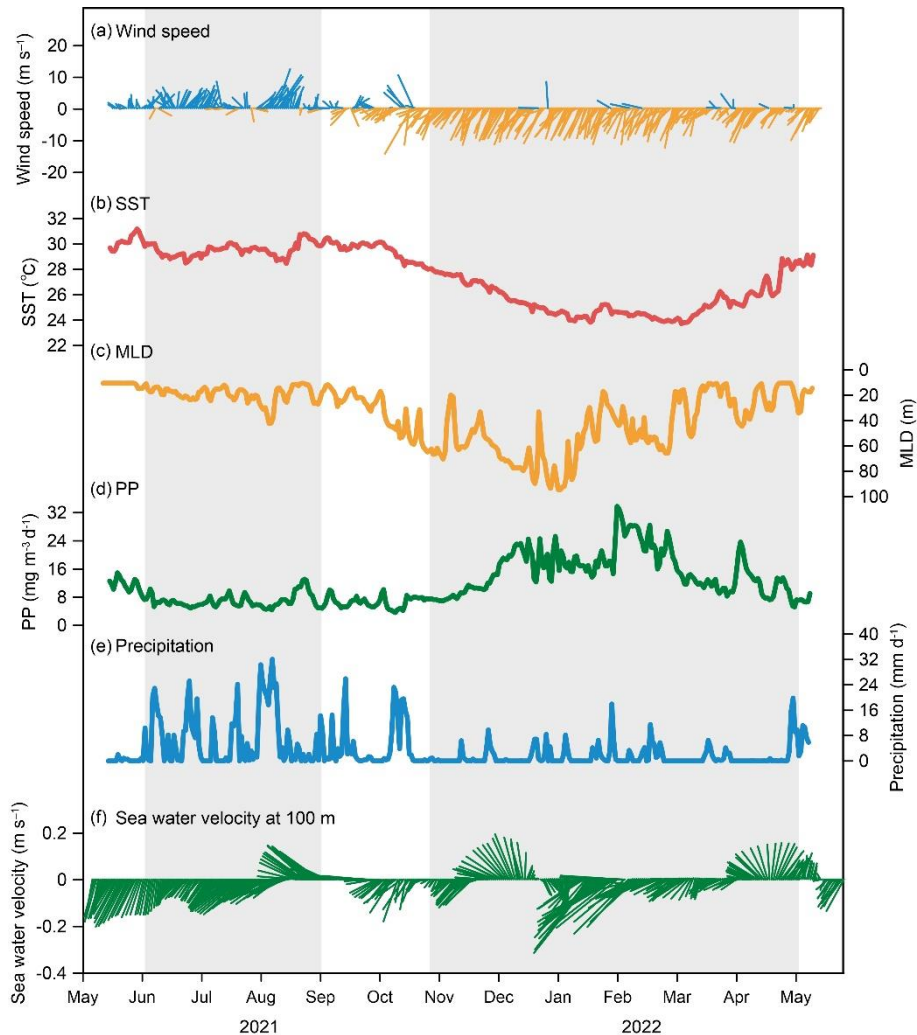
305

Figure 9. Hydrological parameters at the time-series sediment trap mooring TJ-A1B in the northern SCS. (a) wind speed; (b) sea surface temperature (SST); (c) mixed layer depth (MLD); (d) net primary production (PP) of biomass; (e) precipitation; (f) sea water velocity at 100 m.

4~~5~~ Discussion~~s~~

310 **4~~5~~.1 Seasonal variation of POC and FPC export**

Temporal patterns of the POC and the FPC fluxes in the northern SCS exhibited clear seasonal signals with well-defined winter peaks (November to ~~-~~April). The POC flux during this period constituted over 75% of the total annual POC flux (Fig. 10~~9~~a). The FPC flux was also elevated, and the average flux during this period was 2 to 4 times higher than the average flux over the whole deployment period (Fig. 10~~9~~b). ~~Wind speed was also the highest during this period, reaching 8–10 m s⁻¹ (Fig. 9e).~~

315 ~~Meanwhile, the sea surface temperature (SST) declined continuously after November, reaching a minimum (24°C) in January and March (Fig. 9d).~~ During the winter monsoon period, cooling of surface water, along with the strong northeasterly winds resulted in the enhanced vertical mixing, which can be reflected in the variation of the ~~mixed layer depth (~~MLD~~)~~ (Fig. 10c). ~~MLD was typically shallow (<40 m) during spring and summer, increased in autumn and reached its maximum (95 m) in late December (Fig. 9e),~~ MLD was the highest during this period, reaching 95 m, even deeper than the upper nutricline (Wong et

320 al., 2015; Du et al., 2017). High concentrations of ~~primary productivity (~~PP~~)~~ also indicated that the subsurface water provided adequate nutrients to the upper layer, which stimulated the growth of phytoplankton (Fig. 10d~~9f~~). In the northern SCS, Chen et al. (2009) also reported a winter phytoplankton bloom (including *Picoeukaryotes*, *Synechococcus*, and *Prochlorococcus*). The significant increase in PP provided an enhanced food supply and supported high zooplankton biomass, thus resulting in twice the average zooplankton abundance compared to the other seasons (Fig. 2; Li et al., 2004; Tseng et al., 2005; Li et al.,

325 2021). This pattern was consistent with studies in the southern SCS, where higher FPN and FPC fluxes were recorded during the East Asian winter monsoon (Li et al., 2022). Therefore, changes in phytoplankton community structure and zooplankton abundance influenced by the northeast monsoon resulted in a significant increase in the POC and the FPC fluxes. Similarly, in the northern Arabian Sea, fecal pellets were the dominant contributor to particulate matter during the northeast monsoon (Roman et al., 2000; Ramaswamy et al., 2005). In the northeastern Mediterranean Sea, the FPC flux also showed spring peaks

330 during phytoplankton blooms (Carroll et al., 1998). Therefore, although in ~~the~~ oligotrophic seas, the monsoon system can increase the marine primary~~sea surface~~ productivity, which allows for increased zooplankton biomass and promotes the export of carbon from their fecal pellets.
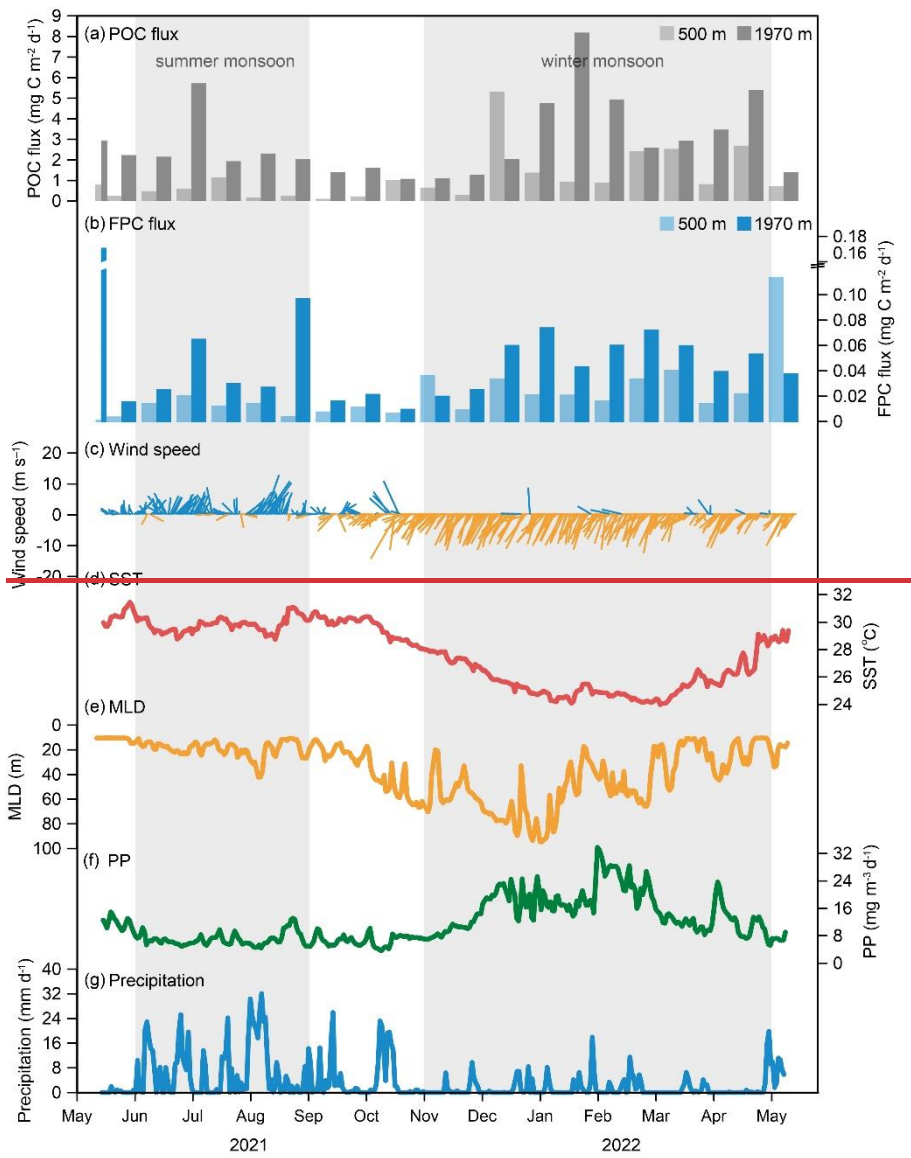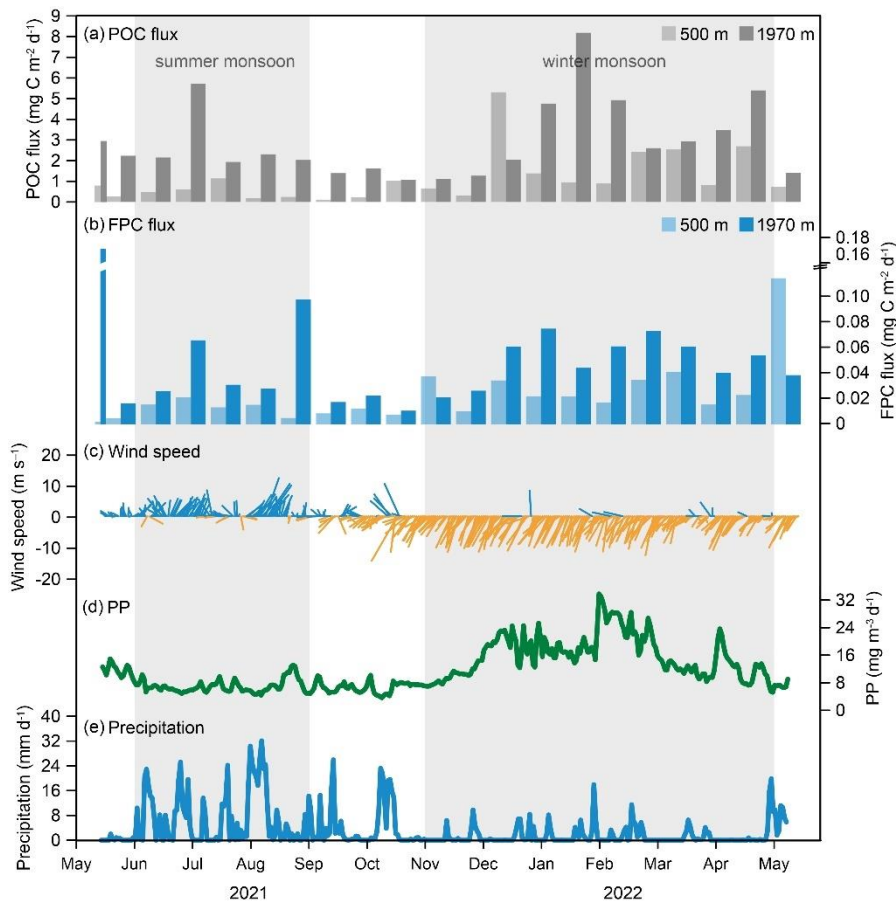
Figure 109. Seasonal variability of POC flux, FPC flux, and three~~five~~ hydrological parameters at the time-series sediment trap mooring TJ-A1B in the northern SCS. (a) POC flux; (b) FPC flux; (c) wind speed; (d) ~~sea surface temperature (SST); (e) mixed layer depth (MLD); (f)~~ net primary production (PP) of biomass; (eg) precipitation.

Secondary peaks in the POC and the FPC fluxes occurred in summer (June to ~~-~~August) (Fig. 109a, ~~and 9~~b). The southwest monsoon, typically accompanied by strong winds in the SCS, was a potential driver. However, from June to July 2021, mean wind speed decreased from 6.7 to 5.4 m s^{-1} (Fig. 109c), with generally high SST (>28°C), which intensified the upper layer stratification. At this time, the MLD was less than 45 m, which was probably insufficient to transport subsurface nutrients to the epipelagic~~uphotic~~ layer. Therefore, the observed increase in the POC and the FPC fluxes cannot be attributed solely to the summer monsoon, but also to rainfall and terrestrial nutrient inputs. Indeed, precipitation in the northern SCS was highly seasonal, with up to 70% concentrated between June and September (Fig. 10e~~9g~~; Zhang et al., 2019). Summer precipitation can bring terrestrial organic matter from land into the ocean, resulting in the increased POC fluxes. This organic matter can also serve as a nutrient supply, contributing to the marine primary productivity, thus increasing zooplankton biomass and FPC

fluxes~~through rivers, and the~~ise additional nutrients ~~can lead to an increase in zooplankton biomass~~ (Fig. 10b~~9g~~; Meyers, 1997; Vizzini et al., 2005~~; Chen et al., 2017~~). In addition, the notably high FPC fluxes at 500 m and 1970 m were observed in May 2021 and May 2022, respectively (Fig. 10~~9~~b). Previous studies have highlighted the annual occurrence of a diatom bloom peak in southwestern Taiwan waters in April (Chen et al., 2016). This may have led to a~~n~~ clear~~obvious~~ increase in zooplankton biomass, which produced a large number of fecal pellets ~~(Carroll et al., 1998)~~. These fecal pellets from southwestern Taiwan are likely ~~have been~~ transported to the northern SCS by deep-sea currents, which coincided with the previously reported high FPC flux recorded in May 2014 (Gao et al., 2020). In summary, the POC and the FPC fluxes in the northern SCS exhibited clear~~obvious~~ seasonal variations, which were primarily controlled by the East Asian monsoon system and seasonal precipitation.

4~~5~~.2 Role of zooplankton repackag~~ing~~e in fecal pellet export

Assemblage of different types and sizes of fecal pellets varied with depth, providing an indication of the repackaging by~~of~~ deep-sea dwelling zooplankton in the water column (Wilson et al., 2008). To better understand the FPC~~fecal pellet carbon~~ export to the deep sea, the biovolume of fecal pellets was converted into carbon content in the following discussion. Admittedly, using the same carbon conversion factor for the whole year and for all fecal pellet shapes and zooplankton producers could lead to uncertainty. Despite this uncertainty, our data still provide adequate information on FPC flux and its contribution to total POC flux in the northern SCS. Cylindrical pellets had the highest carbon content (on average 0.07 µg C pellet^{-1}), which was up to 10 times higher than other pellet types (Fig. 11b~~0~~). The maximum carbon content of cylindrical pellets at 1970 m was 10.62 µg C pellet^{-1}, which was 2.5 times higher than the maximum value recorded at 500 m (4.26 µg C pellet^{-1}). The average carbon content of ellipsoidal pellets increased from 0.01 µg C pellet^{-1} at 500 m to 0.02 µg C pellet^{-1} at 1970 m (Fig. 11a~~0~~). Spherical pellets were the smallest, and they also had higher carbon contents at 1970 m than at 500 m (Fig. 11c~~0~~). These larger pellets may result in a twofold increase in the FPC flux at 1970 m (Table 1; Fig. 10~~9~~b), which might come from the in-situ production of fecal pellets by deep-sea dwelling zooplankton communities. According to the literature~~s~~, ellipsoidal pellets could be attributed to copepods, pteropods, appendicularia, and larvae (González et al., 1994, 2004; Wilson et al., 2008; Wexels Riser et al., 2010; Gleiber et al., 2012). Cylindrical pellets are produced by copepods and euphausiids, and spherical pellets are produced by amphipods, ostracods and small copepods (Beaumont et al., 2002; Wexels Riser et al., 2007; Phillips et al., 2009; Köster et al., 2011). The origin of amorphous fecal pellets is still under debate, as they could be produced by chaetognaths (Wilson et al., 2008) or result from the fragmentation of other-shaped intact fecal pellets (Svensen et al., 2012). In the northern SCS, copepods are the dominant group, with some species (*Chiridius poppei*, *Heterorhabdus abyssalis*, *Scolecithricella valens*, and *Calanoides carinatus*) occurring only between 450 and 1000 m depth (Gong et al., 2017; Li et al., 2021). Larger individuals are mainly distributed in the deeper layers and produce larger fecal pellets (Paffenhöfer and Knowles, 1979; Li et al., 2021). This phenomenon of increased deep-sea fecal pellet flux due to mesopelagic and bathypelagic zooplankton is a common occurrence (Fow~~l~~er et al., 1991; Wassmann et al., 2000; Belcher et al., 2017). Although zooplankton distribution is primarily concentrated within the epipelagic~~uphotic~~ zone (0–200 m), the total zooplankton abundance in the mesopelagic zones may

still be substantial due to the large depth extent of these layers (Gong et al., 2017). Therefore, it is likely that a large amountnumber of fecal pellet production still occurs in the mesopelagic/bathypelagic zones to increase the export of fecal pellets to the deep sea, and these fecal pellets are characterized by strong cycling within the water column.
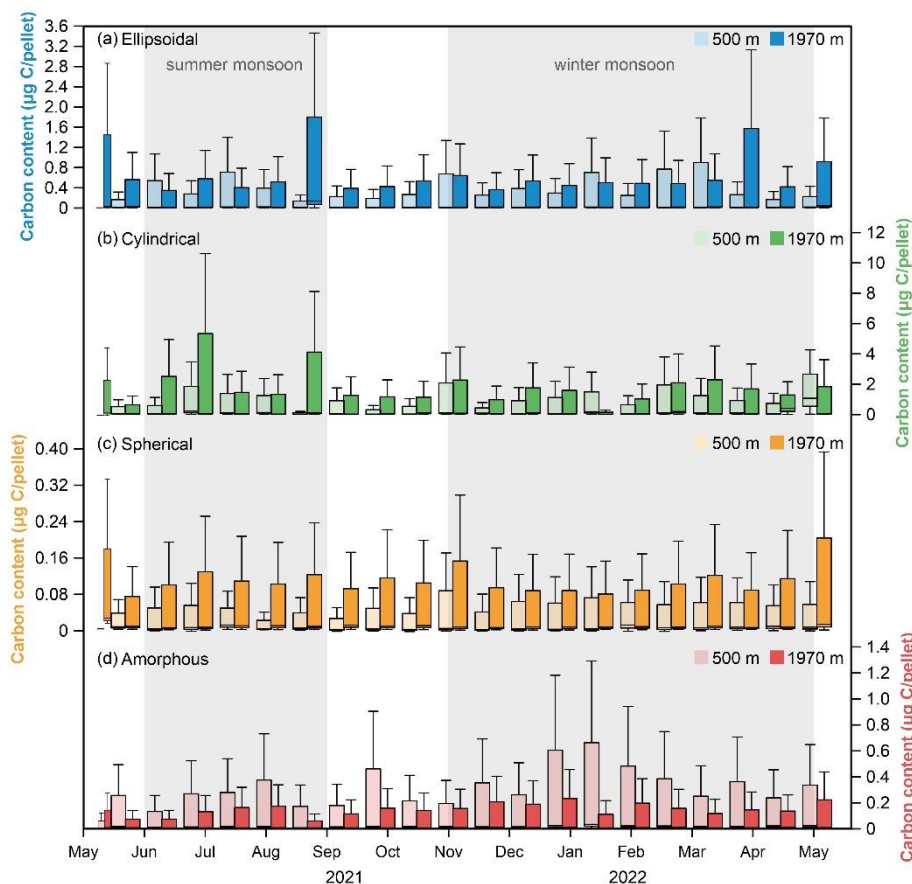
385 **Figure 1110.** Carbon content of four types of fecal pellets at water depths of 500 m and 1970 m at the time-series sediment trap mooring TJ-A1B in the northern SCS. (a) Ellipsoidal pellet; (b) cylindrical pellet; (c) spherical pellet; (d) amorphous pellet.

In addition to the influence of mesopelagic and bathypelagic zooplankton, lateral input by deep-sea currents may also be a
390 significant factor in the increasing export of fecal pellets to the deep sea. Analysis of the internal composition of fecal pellets identified the presence of terrigenous minerals like quartz and clay minerals, with an elemental composition characterized primarily by O, Si, C, Ca, Al, and K (Figs. 4, and 5). The weak correlation between the FPC flux and the POC flux at 1970 m (Fig. 8) also suggested that POC export in the deep northern SCS was influenced by multiple factors including the input from Taiwan rivers (Blattmann et al., 2018, 2019). Previous studies have demonstrated an increasing deep-sea POC flux in the
395 northern SCS due to laterally transported terrestrial organic carbon (Blattmann et al., 2018, 2019; Zhang et al., 2022). Therefore,

the significant increase in the POC flux and the FPC flux in deeper layers may be a result of lateral input via deep-sea currents along the continental slope. This phenomenon has also been observed in the Panama Basin, where Pilskaln and Honjo (1987) reported an increase in the FPC flux from 0.09 mg C m^{-2} d^{-1} at 1268 m to 1.50 mg C m^{-2} d^{-1} at 3769 m. They identified deep-sea currents as a possible driver of the increase in the FPC flux. In summary, lateral transport of deep-sea currents is also likely

400 to lead to increased fluxes of deep fecal pellets.

Conversely, the biovolume and carbon flux of amorphous pellets were significantly reduced at 1970 m compared to the 500 m (Table 1). The average carbon content of amorphous pellets also showed a decrease from 0.02 µg C pellet^{-1} at 500 m to 0.01 µg C pellet^{-1} at 1970 m (Fig. 11d0), indicating the fragmentation of fecal pellets during the sinking process. Previous studies have shown that certain copepod species have distinct feeding behaviors on fecal pellets (Noji et al., 1991). For instance, the

405 species *Oithona similis* is known to frequently engage in coprorhexy or coprochaly (González and Smetacek, 1994). This highly adaptable species, which is widespread throughout the northern SCS and found in all water layers (Gong et al., 2017), and may play a critical role in fecal pellet fragmentation. In the eastern Fram Strait, higher copepod FPC fluxes were detected in the upper water column compared to the lower water column, indicating the effects of re-feeding and decomposition (Lalande et al., 2016). Similarly, studies conducted at K2 station K2 also provided evidence of fecal pellet fragmentation by

410 repackaging of mesopelagic sinking debris (Wilson et al., 2008). These phenomena further support the idea that deep-sea dwelling zooplankton may play a significant role in the repackaging of fecal pellets. Additionally, increased current activity may also lead to fragmentation of fecal pellets. As shown in Fig. 121, the amorphous FPC flux showed a trend of winter peak and summer sub-peak, with the highest value occurring in May 2021. However, the temporal variation in amorphous pellet proportion to the total FPC flux did not show consistency with the amorphous FPC flux (Fig. 121b). Notably, as current

415 velocity increased, the proportion of amorphous pellets to the total FPC flux was significantly higher (~40%), meaning that these pellets exhibited a higher degree of fragmentation (Fig. 121b, and 11c). Therefore, the fragmentation of fecal pellets in the northern SCS shows the joint effect of zooplankton reworking grazing and hydrodynamic changes.
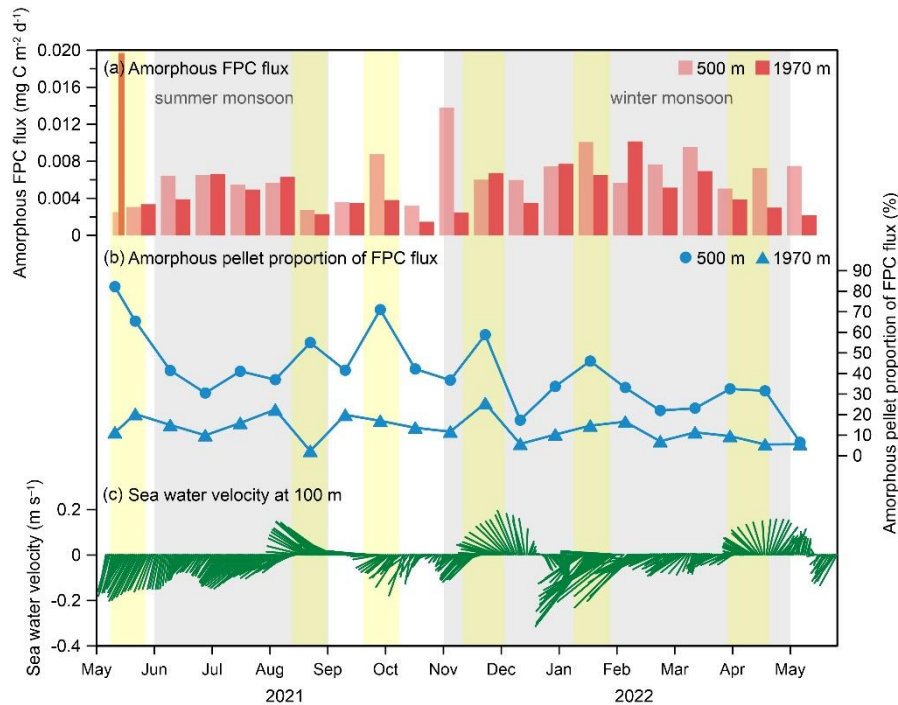
Figure 12~~11~~. Correlation between (a) amorphous FPC flux, (b) amorphous pellet proportion to the total FPC flux, and (c) sea water velocity at 100 m at the time-series sediment trap mooring TJ-A1B in the northern SCS. Yellow shadows display the period with a relatively high proportion of amorphous pellets to the total FPC flux.

4~~5~~.3 Sinking fate of zooplankton fecal pellets

In the northern SCS, various~~able~~ mechanisms affect the carbon export of zooplankton fecal pellets (Fig. 13~~2~~). In the epipelagic~~uphotic~~ zone, zooplankton consume phytoplankton and egest sinking fecal pellets. Phytoplankton cells, zooplankton moults, and fecal pellets together form ~~the~~ larger aggregates. High FPC fluxes are observed during the northeast monsoon period and the summer rainy season. Presence of deep-sea dwelling zooplankton communities and lateral inputs from the slope into the deep basins tend to increase the export of fecal pellet to the deep sea. However, amorphous pellets are fragmented during the sinking process, indicating that surface-produced pellets are likely to be consumed and reworked by zooplankton grazing and fragmented by strong hydrodynamic activities. Also, lateral removal by deep-sea currents can transport fecal pellets away from the northern SCS eventually to different basins. The evolving picture regarding the sinking fate of fecal pellets is therefore a coupling between the marine primary productivity~~surface primary production~~, repackaging and fragmentation by mesopelagic and bathypelagic zooplankton, lateral input and removal by deep-sea currents and hydrodynamically induced fragmentation.
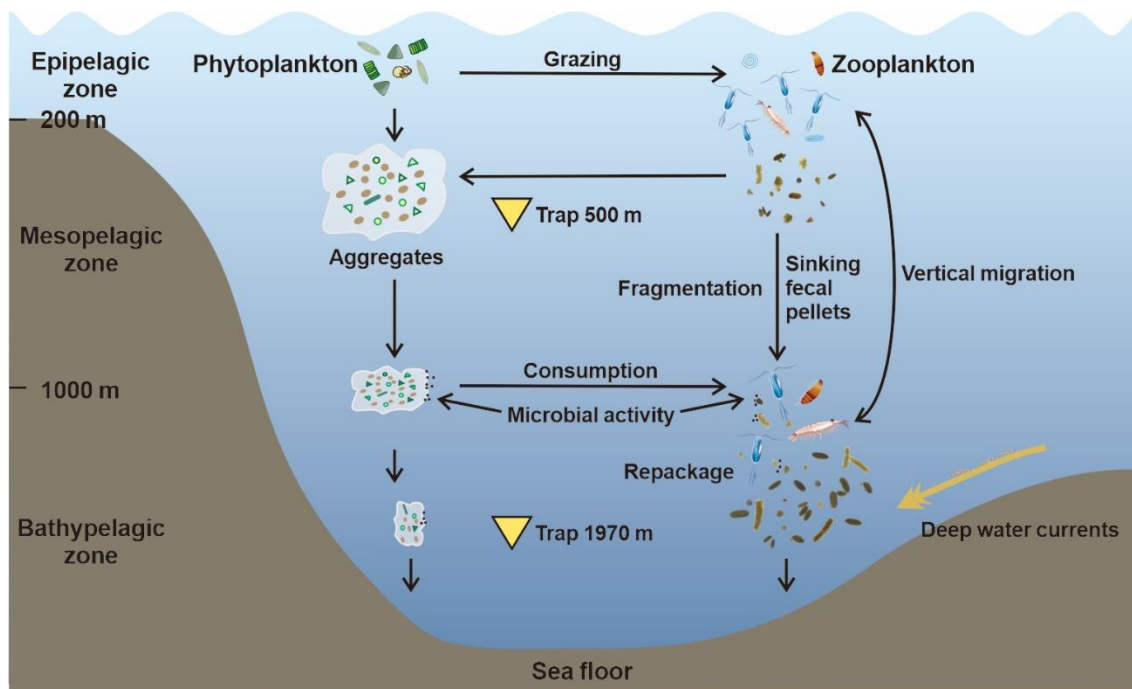
435 **Figure 13~~12~~.** Conceptual graph of the sinking processes regulating the carbon export of fecal pellets in the northern SCS. Yellow triangles show the locations of time-series sediment traps to collect fecal pellets in this study.

Zooplankton fecal pellets were a minor contributor to POC flux in the northern SCS. Fecal pellets contributed an average of 3.4% (range 0.3–15.8%) of the POC flux at 500 m, and 1.9% (range 0.5–5.7%) of the POC flux at 1970 m. These results are
440 similar to those from several other oligotrophic seas (Urrère and Knauer, 1981; Pilskaln and Honjo, 1987; Wassmann et al., 2000; Wilson et al., 2008; Goldthwait and Steinberg, 2008; Shatova et al., 2012). ~~However, compared to the southern SCS (9.0%),~~ ~~T~~the contribution of fecal pellets to the total annual carbon flux was ~~comparatively~~ lower in the northern SCS compared to the southern SCS, possibly due to their higher degree of fragmentation and degradation (Li et al., 2022). After being fragmented, fecal pellets will become small fragments and eventually reach to the sea floor. During the sinking process,
445 they may form larger aggregates with other materials, or they may continue to be degraded and become dissolved organic matter. Even though 87% of the sinking POC in the northern SCS was from marine bio~~genic~~~~spheric~~ origin, the majority may have come from phytoplankton cells such as *Prochlorococcus* and *Synechococcus*, zooplankton mo~~u~~lts, zooplankton carcasses, and large aggregates (Zhang et al., 2019, 2022). Negative correlations between the POC flux and the fecal pellet contribution were observed, indicating that during periods of low POC flux, fecal pellets may play a proportionally larger role in deep-sea
450 carbon export (Fig. 8). In contrast, during periods of high POC flux, aggregates composed of diatoms, dinoflagellate flocs, fecal pellets, and other debris appeared to be the major contributors (Fig. 3). Wilson et al. (2013) found that during periods of low POC flux in the northeast Pacific, fecal pellets also accounted for a greater proportion of deep-sea POC flux. This negative

correlation between the FPC flux and the POC flux may be a common characteristic of particulate fluxes in the deep ocean (Wilson et al., 2013). In the northern SCS, the FPC flux was relatively low, with a high abundance of amorphous pellets and significantly low FPC/POC ratios, which may indicate a low efficiency BCP with a weak carbon sink effect.

Although the contribution of fecal pellets to the total carbon flux in the northern SCS is quantitatively low (0.3–15.8%), detailed analyses of the spatiotemporal variations in fecal pellet fluxes can provide significant insights into the processes controlling fecal pellet production, sinking, and reworking. Linking fecal pellet fluxes to seasonal and oceanographic dynamics can provide new insights for investigating the efficiency of BCP in the SCS, and greatly enhance our understanding of the biogeochemical processes that influence the export of organic carbon to the deep sea. Additional research is needed to determine the presence of fecal pellets at the sediment–-water interface, and to further explore the sinking and burial processes of POC in the deep sea, from sinking particles to sediment cores.

56 Conclusions

Characteristics, internal structure, quantity, and carbon content of zooplankton fecal pellets were investigated in the northern SCS to quantify the numerical and carbon fluxes of fecal pellets and to explore the process of fecal pellet sinking in the tropical marginal sea. Our conclusions are as follows:

1. Seasonal variations in the FPN and the FPC fluxes showed distinct peaks from November to April and from June to August. Strong northeast monsoon and surface water cooling led to the mixing of the upper water column, importing nutrients from subsurface into the epipelagiceuphotic layer, stimulating phytoplankton growth and increasing FPC flux in winter. Additionally, the FPC fluxes were also high in summer due to heavy precipitation that brought terrestrial nutrients into the sea.

2. Zooplankton fecal pellet fluxes were twice as highhigher at 1970 m than at 500 m. The occurrence of larger ellipsoidal, cylindrical, and spherical pellets at 1970 m provided evidence for repackaging and in -situ production of mesopelagic/bathypelagic zooplankton communities, and lateral input by deep-sea currents. Amorphous pellets were abundant and their biovolume decreased by half at 1970 m compared to 500 m, indicating that these fecal pellets were subject to fragmentation during sinking, possibly due to the impacts of zooplankton grazing and strong current disturbance.

3. The sinking process of fecal pellets is controlled by a combination of marine primarysea surface productivity, mesopelagic and bathypelagic zooplankton repackaging, as well as current activities. Although the contribution of fecal pellets to the deep-sea carbon flux is relatively low in the northern SCS, fecal pellets still play a variable but indispensable role in the vertical carbon export.

Data availability

The data involved in this study have been archived~~are underway of archiving~~ at the PANGAEA database (https://doi.pangaea.de/10.1594/PANGAEA.962713~~https://issues.pangaea.de/browse/PDI-35447~~). ~~They are provided as supporting materials during the reviewing process.~~

Supplement

The supplement related to this article is available online.

Author contributions

ZL designed the study and obtained the funding. HW carried out the measurements and wrote the original draft with helps of JL and BL. HW, ZL, JL, BL, and YZ contributed to data interpretation and manuscript writing. ZL, JL, BL, YZ, XZ, JC, JZ, HS, and WW participated in mooring deployment/recovery cruises.

Competing interests

The contact author has declared that none of the authors has any competing interests.

Disclaimer

Publisher's note: Copernicus Publications remains neutral with regard to jurisdictional claims in published maps and institutional affiliations.

Acknowledgments

We would like to thank Chen Ling, Longwei Wu, and Lingmin Zhang from Tongji University for the assistance during mooring deployment/recovery cruise and laboratory analysis. We especially thank Dr. Marcel van der Meer (Editor) and two anonymous referees for their comments, which greatly improved this manuscript.

Financial support

This work has been supported by the National Natural Science Foundation of China (42130407, 42188102).

References

Beaumont, K. L., Nash, G. V., and Davidson, A. T.: Ultrastructure, morphology and flux of microzooplankton faecal pellets in an east Antarctic fjord, Mar. Ecol. Prog. Ser., 245, 133–148, https://doi.org/10.3354/meps245133, 2002.

Belcher, A., Manno, C., Ward, P., Henson, S. A., Sanders, R., and Tarling, G. A.: Copepod faecal pellet transfer through the meso-and bathypelagic layers in the Southern Ocean in spring, Biogeosciences, 14, 1511–1525, https://doi.org/10.5194/bg-14-1511-2017, 2017.

Blattmann, T. M., Liu, Z., Zhang, Y., Zhao, Y., Haghipour, N., Montlucon, D. B., Plotze, M., and Eglinton, T. I.: Mineralogical control on the fate of continentally derived organic matter in the ocean, Science, 366, 742–745, https://doi.org/10.1126/science.aax5345, 2019.

Blattmann, T. M., Zhang, Y., Zhao, Y., Wen, K., Lin, S., Li, J., Wacker, L., Haghipour, N., Plotze, M., Liu, Z., and Eglinton, T. I.: Contrasting Fates of Petrogenic and Biospheric Carbon in the South China Sea, Geophys. Res. Lett., 45, 9077–9086, https://doi.org/10.1029/2018gl079222, 2018.

Boyd, P.W., Claustre, H., Levy, M., Siegel, D. A., and Weber, T.: Multi-faceted particle pumps drive carbon sequestration in the ocean, Nature, 568, 327–335, https://doi.org/10.1038/s41586-019-1098-2, 2019.

Cao, Z., Yang, W., Zhao, Y., Guo, X., Yin, Z., Du, C., Zhao, H., and Dai, M.: Diagnosis of CO_2 dynamics and fluxes in global coastal oceans, Natl. Sci. Rev., 7, 786–797, https://doi.org/10.1093/nsr/nwz105, 2020.

Carroll, M. L., Miquel, J. C., and Fowler, S. W.: Seasonal patterns and depth-specific trends of zooplankton fecal pellet fluxes in the Northwestern Mediterranean Sea, Deep-Sea Res. I, 45, 1303–1318, https://doi.org/10.1016/S0967-0637(98)00013-2, 1998.

Caruso, M. J., Gawarkiewicz, G. G., and Beardsley, R. C.: Interannual variability of the Kuroshio intrusion in the South China Sea, J. Oceanogr., 62, 559–575, https://doi.org/10.1007/s10872-006-0076-0, 2006.

Chen, B., Liu, H., Landry, M. R., Dai, M., Huang, B., and Sun, J.: Close coupling between phytoplankton growth and microzooplankton grazing in the western South China Sea, Limnol. Oceanogr., 54, 1084–1097, https://doi.org/10.4319/lo.2009.54.4.1084, 2009.

Chen, C., Mao, Z., Han, G., Zhu, Q., Gong, F., and Wang, T.: Latitudinal and interannual variations of the spring phytoplankton bloom peak in the East Asian marginal seas, Acta. Oceanol. Sin., 35, 81–88, https://doi.org/10.1007/s13131-016-0867-0, 2016.

Chen, F., Chen C., Zhou, F., Lao, Q., Zhu, Q., and Zhang, S.: Nutrients in atmospheric wet deposition in the Zhanjiang Bay. (in Chinese), China Environmental Science, 37, 2055–2063, 2017.

Chen, J., Zheng, L., Wiesner, M. G., Chen, R., Zheng, Y., and Wong, H.: Estimations of primary production and export production in the South China Sea based on sediment trap experiments, Chinese. Sci. Bull., 43, 583–586, https://doi.org/10.1007/Bf02883645, 1998.

Chen, Y.-L. L.: Spatial and seasonal variations of nitrate-based new production and primary production in the South China Sea, Deep-Sea Res. I, 52, 319–340, https://doi.org/10.1016/j.dsr.2004.11.001, 2005.

535 Chu, P., and Wang, G.: Seasonal variability of thermohaline front in the central South China Sea, J. Oceanogr., 59, 65–78, https://doi:10.1023/a:1022868407012, 2003.

Du, C., Liu, Z., Kao, S.-J., and Dai, M.: Diapycnal Fluxes of Nutrients in an Oligotrophic Oceanic Regime: The South China Sea, Geophys. Res. Lett., 44, 11510–11518, https://doi.org/10.1002/2017GL074921, 2017.

Du, F., Wang, X., Gu, Y., Yu, J., Wang, L., Ning, J., Lin, Q., Jia, X., and Yang, S.: Vertical distribution of zooplankton in

540 the continental slope southwest of Nansha Islands, South China Sea. (in Chinese), Acta. Oceanol. Sin., 36, 94–103, https://doi.org/10.3969/j. issn.0253-4193.2014.06.012, 2014.

Fowler, S. W. and Knauer, G. A.: Role of Large Particles in the Transport of Elements and Organic-Compounds through the Oceanic Water Column, Prog. Oceanogr., 16, 147–194, https://doi.org/10.1016/0079-6611(86)90032-7, 1986.

Fowler, S. W., Small, L. F., and Larosa, J.: Seasonal Particulate Carbon Flux in the Coastal Northwestern Mediterranean-

545 Sea, and the Role of Zooplankton Fecal Matter, Oceanol. Acta., 14, 77–85, 1991.

Gao, M., Huang, B., Liu, Z., Zhao, Y., and Zhang, Y.: Observations of marine snow and fecal pellets in a sediment trap mooring in the northern South China Sea, Acta. Oceanol. Sin., 39, 141–147, https://doi.org/10.1007/s13131-020-1561-9, 2020.

Ge, R., Chen, H., Zhuang, Y., and Liu, G.: Active Carbon Flux of Mesozooplankton in South China Sea and Western

550 Philippine Sea, Frontiers in Marine Science, 8, https://doi.org/10.3389/fmars.2021.697743, 2021.

Gleiber, M. R., Steinberg, D. K., and Ducklow, H. W.: Time series of vertical flux of zooplankton fecal pellets on the continental shelf of the western Antarctic Peninsula, Mar. Ecol. Prog. Ser., 471, 23–36, https://doi.org/10.3354/meps10021, 2012.

Goldthwait, S. A. and Steinberg, D. K.: Elevated biomass of mesozooplankton and enhanced fecal pellet flux in cyclonic and

555 mode-water eddies in the Sargasso Sea, Deep-Sea Res. Pt. II, 55, 1360–1377, https://doi.org/10.1016/j.dsr2.2008.01.003, 2008.

Gong, Y., Yang, Y., Fang, J., Cai, Y., Xu, S., and Chen, Z.: Spatial distribution of zooplankton in continental slope of northern South China Sea in summer, South China Fisheries Science, 13, 8–15. (in Chinese), https://doi.org/10.3969/j.issn.2095-0780.2017.05.002, 2017.

560 González~~Gonzalez~~, H. E. and Smetacek, V.: The possible role of the cyclopoid copepod *Oithona* in retarding vertical flux of zooplankton fecal material, Mar. Ecol. Prog. Ser., 113, 233–246, https://doi.org/10.3354/meps113233, 1994.

González~~Gonzalez~~, H. E., Daneri, G., Iriarte, J. L., Yannicelli, B., Menschel, E., Barria, C., Pantoja, S., and Lizarraga, L.: Carbon fluxes within the epipelagic zone of the Humboldt Current System off Chile: The significance of euphausiids and diatoms as key functional groups for the biological pump, Prog. Oceanogr., 83, 217–227, 1

565 https://doi.org/10.1016/j.pocean.2009.07.036, 2009.

González~~Gonzalez~~, H. E., González~~Gonzalez~~, S. R., and Brummer, G. J. A.: Short-Term ~~Short-term~~ sedimentation pattern of zooplankton, feces and microplankton at a permanent station in the Bjornafjorden (Norway) during April–May 1992, Mar. Ecol. Prog. Ser., 105, 31–45, https://doi. org/10.3354/meps105031, 1994.

González, H. E., Hebbeln, D., Iriarte, J. L., and Marchant, M.: Downward fluxes of faecal material and microplankton at 2300m depth in the oceanic area off Coquimbo (30°S), Chile, during 1993–1995, Deep-Sea Res. Pt. II, 51, 2457–2474, https://doi.org/10.1016/j.dsr2.2004.07.027, 2004.

González~~Gonzalez~~, H. E., Ortiz, V. C., and Sobarzo, M.: The role of faecal material in the particulate organic carbon flux in the northern Humboldt Current, Chile (23°S), before and during the 1997–1998 El Niño, J. Plankton. Res., 22, 499–529, https://doi.org/10.1093/ plankt/22.3.499, 2000.

Juul-Pedersen, T., Nielsen, T. G., Michel, C., Moller, E. F., Tiselius, P., Thor, P., Olesen, M., Selander, E., and Gooding, S.: Sedimentation following the spring bloom in Disko Bay, West Greenland, with special emphasis on the role of copepods, Mar. Ecol. Prog. Ser., 314, 239–255, https://doi.org/10.3354/meps314239, 2006.

Kobari, T., Akamatsu, H., Minowa, M., Ichikawa, T., Iseki, K., Fukuda, R., and Higashi, M.: Effects of the Copepod Community Structure on Fecal Pellet Flux in Kagoshima Bay, a Deep, Semi-Enclosed Embayment, J. Oceanogr., 66, 673–684, https://doi.org/10.1007/ s10872-010-0055-3, 2010.

Kobari, T., Nakamura, R., Unno, K., Kitamura, M., Tanabe, K., Nagafuku, H., Niibo, A., Kawakami, H., Matsumoto, K., and Honda, M. C.: Seasonal variability in carbon demand and flux by mesozooplankton communities at subarctic and subtropical sites in the western North Pacific Ocean, J. Oceanogr., 72, 403–418, https://doi.org/10.1007/s10872-015-0348-7, 2016.

Köster~~Koster~~, M., Sietmann, R., Meuche, A., and Paffenhöfer~~Paffenhofer~~, G. A.: The ultrastructure of a doliolid and a copepod fecal pellet, J. Plankton. Res., 33, 1538–1549, https://doi.org/10.1093/plankt/fbr053, 2011.

Kumar, R. G., Strom, K. B., and Keyvani, A.: Floc properties and settling velocity of San Jacinto estuary mud under variable shear and salinity conditions, Cont. Shelf. Res., 30, 2067–2081, https://doi.org/10.1016/j.csr.2010.10.006, 2010.

Lalande, C., Nöthig, E.-M., Bauerfeind, E., Hardge, K., Beszczynska- Möller, A., and Fahl, K.: Lateral supply and downward export of particulate matter from upper waters to the seafloor in the deep eastern Fram Strait, Deep-Sea Res. Pt. I, 114, 78–89, https://doi.org/10.1016/j.dsr.2016.04.014, 2016.

Le Moigne, F. A. C.: Pathways of Organic Carbon Downward Transport by the Oceanic Biological Carbon Pump, Frontiers in Marine Science, 6, 634, https://doi.org/10.3389/fmars.2019.00634, 2019.

Li, C., Jia, X., and Cai, W.: Diversity of marine zooplankton in the north of South China Sea (in Chinese), Journal of Fishery Sciences of China, 11, 139–146, 2004.

Li, H., Wiesner, M. G., Chen, J., Ling, Z., Zhang, J., and Ran, L.: Long-term variation of mesopelagic biogenic flux in the central South China Sea: Impact of monsoonal seasonality and mesoscale eddy, Deep-Sea Res. Pt. I, 126, 62–72, https://doi.org/10.1016/j.dsr.2017.05.012, 2017.

Li, J., Liu, Z., Lin, B., Zhao, Y., Cao, J., Zhang, X., Zhang, J., Ling, C., Ma, P., and Wu, J.: Zooplankton fecal pellet

600   characteristics and contribution to the deep-sea carbon export in the southern South China Sea, J. Geophys. Res-
Oceans., 127, https://doi.org/10.1029/2022JC019412, 2022.

Li, K., Ren, Y., Ke, Z., Li, G., and Tan, Y.: Vertical distributions of epipelagic and mesopelagic zooplankton in the
continental slope of the northeastern South China Sea (in Chinese), Journal of Tropical Oceanography, 40, 61–73,
https://doi.org/10.11978/2020061, 2021.

605   Li, K., Yin, J., Huang, L., Tan, Y., and Lin, Q.: A comparison of the zooplankton community in the Bay of Bengal and South
China Sea during April–May, 2010, J. Ocean. U. China., 16, 1206–1212, https://doi.org/10.1007/s11802-017-3229-4,
2017.

Liu, K.-K., Chao, S.-Y., Shaw, P.-T., Gong, G.-C., Chen, C.-C., and Tang, T.: Monsoon-forced chlorophyll distribution and
primary production in the South China Sea: observations and a numerical study, Deep-Sea Res. Pt. I, 49, 1387–1412,

610   https://doi.org/10.1016/s0967-0637(02)00035-3, 2002.

Liu, K.-K., Kao, S.-J., Hu, H.-C., Chou, W.-C., Hung, G.-W., and Tseng, C.-M.: Carbon isotopic composition of suspended
and sinking particulate organic matter in the northern South China Sea—From production to deposition, Deep-Sea Res.
Pt. II, 54, 1504–1527, https://doi.org/10.1016/j.dsr2.2007.05.010, 2007.

Liu, Z., Colin, C., Li, X., Zhao, Y., Tuo, S., Chen, Z., Siringan, F. P., Liu, J., Huang, C., You, C., and Huang, K.: Clay

615   mineral distribution in surface sediments of the northeastern South China Sea and surrounding fluvial drainage basins:
Source and transport, Mar. Geol., 277, 48–60, https://doi.org/10.1016/j.margeo.2010.08.010, 2010.

Liu, Z., Zhao, Y., Colin, C., Stattegger, K., Wiesner, M. G., Huh, C.-A., Zhang, Y., Li, X., Sompongchaiyakul, P., You, C.,
Huang, C., Liu, J., Siringan, F. P., Le, K. P., Sathiamurthy, E., Hantoro, W. S., Liu, J., Tuo, S., Zhao, S., Zhou, S., He,
Z., Wang, Y., Bunsomboonsakul, S., and Li, Y.: Source-to-sink transport processes of fluvial sediments in the South

620   China Sea, Earth-Sci. Rev., 153, 238–273, https://doi.org/10.1016/j.earscirev.2015.08.005, 2016.

Manno, C., Stowasser, G., Enderlein, P., Fielding, S., and Tarling, G. A.: The contribution of zooplankton faecal pellets to
deep-carbon transport in the Scotia Sea (Southern Ocean), Biogeosciences, 12, 1955–1965, https://doi.org/10.5194/bg-
12-1955-2015, 2015.

Meyers, P. A.: Organic geochemical proxies of paleoceanographic, paleolimnologic, and paleoclimatic processes, Org.

625   Geochem. 27, 213–250, https://doi.org/10.1016/S0146-6380(97)00049-1, 1997.

Miquel, J. C., Gasser, B., Martín, J., Marec, C., Babin, M., Fortier, L., and Forest, A.: Downward particle flux and carbon
export in the Beaufort Sea, Arctic Ocean; the role of zooplankton, Biogeosciences, 12, 5103–5117,
https://doi.org/10.5194/bg-12-5103-2015, 2015.

Noji, T. T., Estep, K. W., Macintyre, F., and Norrbin, F.: Image analysis of fecal material grazed upon by 3 species of

630   copepods: Evidence for coprorhexy, coprophagy and coprochaly, J. Mar. Biol. Assoc. UK., 71, 465–480,
https://doi.org/10.1017/s0025315400051717, 1991.

Paffenhöfer, G. A., and Knowles, S. C.: Ecological implications of fecal pellet size, production and consumption by copepods, J. Mater. Res., 37, 35–49, 1979.

Phillips, B., Kremer, P., and Madin, L. P.: Defecation by Salpa thompsoni and its contribution to vertical flux in the Southern Ocean, Mar. Biol., 156, 455–467, https://doi.org/10.1007/s00227-008-1099-4, 2009.

Pilskaln, C. H. and Honjo, S.: The fecal pellet fraction of biogeochemical particle fluxes to the deep sea, Global. Biogeochem. Cy., 1, 31–48, https://doi.org/10.1029/GB001i001p00031, 1987.

Qiu, Y., Laws, E. A., Wang, L., Wang, D., Liu, X., and Huang, B.: The potential contributions of phytoplankton cells and zooplankton fecal pellets to POC export fluxes during a spring bloom in the East China Sea, Cont. Shelf. Res., 167, 32–45, https://doi.org/10.1016/j.csr.2018.08.001, 2018.

Ramaswamya, V., Sarin, M. M., and Rengarajan, R.: Enhanced export of carbon by salps during the northeast monsoon period in the northern Arabian Sea, Deep-Sea Res. Pt. II, 52, 1922–1929, https://doi.org/10.1016/j.dsr2.2005.05.005, 2005.

Ren, Y., Yin, J., Tan, Y., Liu, H., Yu, L., and Li, K.: Monsoon-driven seasonal and spatial distribution of the copepod community along the northwest continental shelf of the South China Sea, J. Marine. Syst., 218, 103529, https://doi.org/10.1016/j.jmarsys.2021.103529, 2021.

Roman, M. R., and Gauzens, A. L.: Copepod grazing in the equatorial Pacific, Limnol. Oceanogr., 42, 623–634, https://doi.org/10.4319/lo.1997.42.4.0623, 1997.

Roman, M., Smith, S., Wishner, K., Zhang, X. S., and Gowing, M.: Mesozooplankton production and grazing in the Arabian Sea, Deep-Sea Res. Pt. II, 47, 1423–1450, https://doi.org/10.1016/s0967-0645(99)00149-6, 2000.

Schlitzer, R.: Ocean data view, Retrieved from http://odv.awi.de, 2023.

Shatova, O., Koweek, D., Conte, M. H., and Weber, J. C.: Contribution of zooplankton fecal pellets to deep ocean particle flux in the Sargasso Sea assessed using quantitative image analysis, J. Plankton. Res., 34, 905–921, https://doi.org/10.1093/plankt/ fbs053, 2012.

Steinberg, D. K. and Landry, M. R.: Zooplankton and the ocean carbon cycle, Ann. Rev. Mar. Sci., 9, 413–444, https://doi.org/10.1146/annurev-marine-010814-015924, 2017.

Stukel, M. R., Ohman, M. D., Benitez-Nelson, C. R., and Landry, M. R.: Contributions of mesozooplankton to vertical carbon export in a coastal upwelling system, Mar. Ecol. Prog. Ser., 491, 47–65, https://doi.org/10.3354/meps10453, 2013.

Su, J.: Overview of the South China Sea circulation and its influence on the coastal physical oceanography near the Pearl River Estuary, Cont. Shelf. Res., 24, 1745–1760, https://doi.org/10.1016/j.csr.2004.06.005, 2004.

Sun, J. and Liu, D.: Geometric models for calculating cell biovolume and surface area for phytoplankton, J. Plankton. Res., 25, 1331–1346, https://doi.org/10.1093/plankt/fbg096, 2003.

Svensen, C., Riser, C. W., Reigstad, M., and Seuthe, L.: Degradation of copepod faecal pellets in the upper layer: role of microbial community and Calanus finmarchicus, Mar. Ecol. Prog. Ser., 462, 39–49, https://doi.org/10.3354/meps09808, 2012.

Taylor, G. T.: Variability in the vertical flux of microorganisms and biogenic material in the epipelagic zone of a North Pacific central gyre station, Deep-Sea Res. Pt. I, 36, 1287–1308, https://doi.org/10.1016/0198-0149(89)90084-8, 1989.

Tseng, C.-M., Wong, G. T. F., Lin, I.-I., Wu, C.-R., and Liu, K.-K.: A unique seasonal pattern in phytoplankton biomass in low-latitude waters in the South China Sea, Geophys. Res. Lett., 32, L08608, https://doi.org/10.1029/2004gl022111, 2005.

Turner, J. T.: Zooplankton fecal pellets, marine snow and sinking phytoplankton blooms, Aquat. Microb. Ecol., 27, 57–102, https://doi.org/10.3354/ame027057, 2002.

Turner, J. T.: Zooplankton fecal pellets, marine snow, phytodetritus and the ocean's biological pump, Prog. Oceanogr., 130, 205–248, https://doi.org/10.1016/j.pocean.2014.08.005, 2015.

Urban-Rich, J., Hansell, D. A., and Roman, M. R.: Analysis of copepod fecal pellet carbon using a high temperature combustion method, Mar. Ecol. Prog. Ser., 171, 199–208, https://doi.org/10.3354/meps171199, 1998.

Urrère, M. A. and Knauer, G. A.: Zooplankton fecal pellet fluxes and vertical transport of particulate organic material in the pelagic environment, J. Plankton. Res., 3, 369–387, https://doi.org/10.1093/plankt/3.3.369, 1981.

Viitasalo, M., Rosenberg, M., Heiskanen, A.-S., and Koski, M.: Sedimentation of copepod fecal material in the coastal northern Baltic Sea: Where did all the pellets go? Limnol. Oceanogr., 44, 1388–1399, https://doi.org/10.4319/lo.1999.44.6.1388, 1999.

Vizzini, S., Savona, B., Caruso, M. F., Savona, A., and Mazzola, A.: Analysis of stable carbon and nitrogen isotopes as a tool for assessing the environmental impact of aquaculture: a case study from the western Mediterranean, Aquacult. Int., 13, 157–165, https://doi.org/10.1007/s10499-004-9023-5, 2005.

Wang, P. and Li, Q. (Eds.): Oceanographical and geological background, in: The South China Sea: Paleoceanography and sedimentology, Developments in Paleoenvironmental Research, Springer, The Netherlands, 25–49, https://doi.org/10.1007/978-1-4020-9745-4_1, 2009.

Wassmann, P., Ypma, J. E., and Tselepides, A.: Vertical flux of faecal pellets and microplankton on the shelf of the oligotrophic Cretan Sea (NE Mediterranean Sea), Prog. Oceanogr., 46, 241–258, https://doi.org/10.1016/s0079-6611(00)00021-5, 2000.

Wexels Riser, C., Reigstad, M., and Wassmann, P.: Zooplankton-mediated carbon export: A seasonal study in a northern Norwegian fjord, Mar. Biol. Res., 6, 461–471, https://doi.org/10.1080/17451000903437067, 2010.

Wexels Riser, C., Reigstad, M., Wassmann, P., Arashkevich, E., and Falk-Petersen, S.: Export or retention? Copepod abundance, faecal pellet production and vertical flux in the marginal ice zone through snap shots from the northern Barents Sea, Polar. Biol., 30, 719–730, https://doi.org/10.1007/s00300-006-0229-z, 2007.

Wilson, S. E., Ruhl, H. A., and Smith, K. L.: Zooplankton fecal pellet flux in the abyssal northeast Pacific: A 15 year time-series study, Limnol. Oceanogr., 58, 881–892, https://doi.org/10.4319/lo.2013.58.3.0881, 2013.

Wilson, S. E., Steinberg, D. K., and Buesseler, K. O.: Changes in fecal pellet characteristics with depth as indicators of

700   zooplankton repackaging of particles in the mesopelagic zone of the subtropical and subarctic North Pacific Ocean, Deep-Sea Res. Pt. II, 55, 1636–1647, https://doi.org/10.1016/j.dsr2.2008.04.019, 2008.

Wong, G. T. F., Pan, X., Li, K.-Y., Shiah, F.-K., Ho, T.-Y., and Guo, X.: Hydrography and nutrient dynamics in the Northern South China Sea Shelf-sea (NoSoCS), Deep-Sea Res. Pt. II, 117, 23–40, https://doi.org/10.1016/j.dsr2.2015.02.023, 2015.

705 Zhang, J., Li, H., Wiesner, M. G., Eglinton, T. I., Haghipour, N., Jian, Z., and Chen, J.: Carbon isotopic constraints on basin-scale vertical and lateral particulate organic carbon dynamics in the northern South China Sea, J. Geophys. Res-Oceans., 127, e2022JC018830, https://doi.org/10.1029/2022JC018830, 2022.

Zhang, J., Li, H., Xuan, J., Wu, Z., Yang, Z., Wiesner, M. G., and Chen, J.: Enhancement of mesopelagic sinking particle fluxes due to upwelling, aerosol deposition, and monsoonal influences in the northwestern South China Sea, J.

710   Geophys. Res-Oceans., 124, 99–112, https://doi.org/10.1029/2018jc014704, 2019.

Zhao, Y., Liu, Z., Zhang, Y., Li, J., Wang, M., Wang, W., and Xu, J.: In situ observation of contour currents in the northern South China Sea: Applications for deepwater sediment transport, Earth. Planet. Sc. Lett., 430, 477–485, https://doi.org/10.1016/j.epsl.2015.09.008, 2015.